専門分野「計算固体力学（Computational Solid Mechanics）」

材料と構造のマルチフィールド・マルチスケール力学問題を対象として、有限要素法などの数値シミュレーション手法の開発と工業設計解析および先端テクノロジーへの応用に関する研究を行なってきた。

(1)計算構造工学：非線形・マルチフィールド構造解析法の開発

(2)計算損傷力学：材料損傷・構造寿命のメソ力学評価法の開発

①連続体損傷力学に基づく延性・脆性固体の計算損傷力学の展開
②不連続体力学モデルによる延性・脆性固体の計算メソ力学手法の開発
③マクロ・メソ・ミクロスケールに渡るマルチスケール材料解析法の構築
④損傷力学に基づく数値材料試験法の開発と構造寿命予測への適用
⑤損傷力学の拡張による自己修復材料（耐熱鋼、高分子材料）の計算モデリング

(3)計算機能材料工学：先端機能材料とアクチュエータ/センサの計算モデリング

メソ解析に基づくマイクロクラッキング脆性固体の計算損傷力学モデル
[24.都井・諸1993a, 25.同1993b]

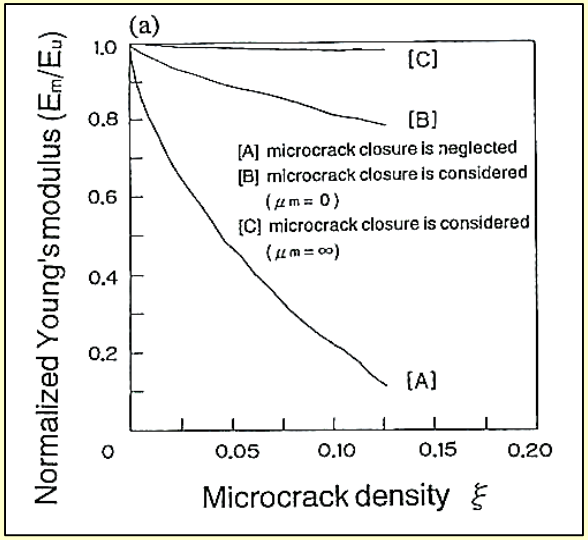

Young's modulus versus microcrack density under compressive loading

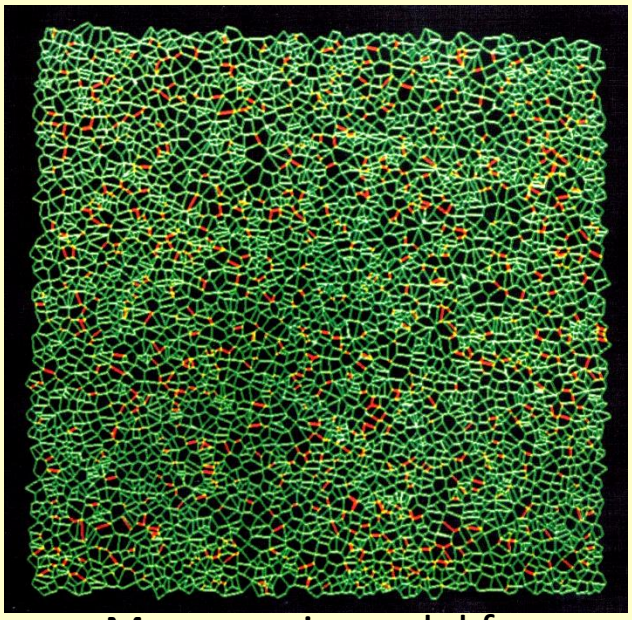

Mesoscopic model for brittle microcracking solids (4453 elements)

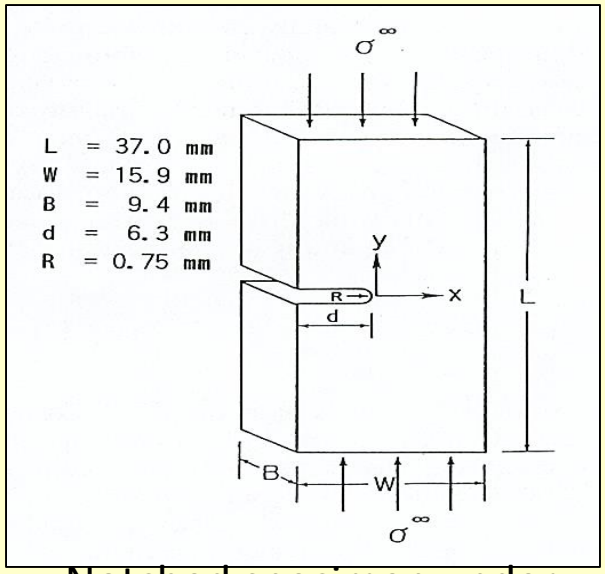

Notched specimen under compressive loading

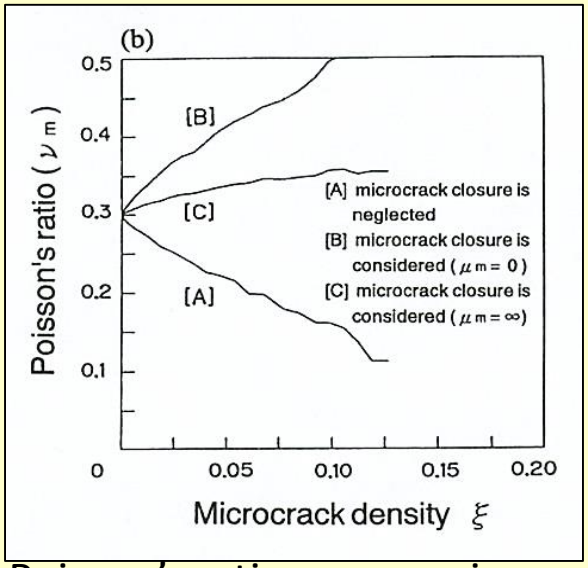

Poisson's ratio versus microcrack density under compressive loading

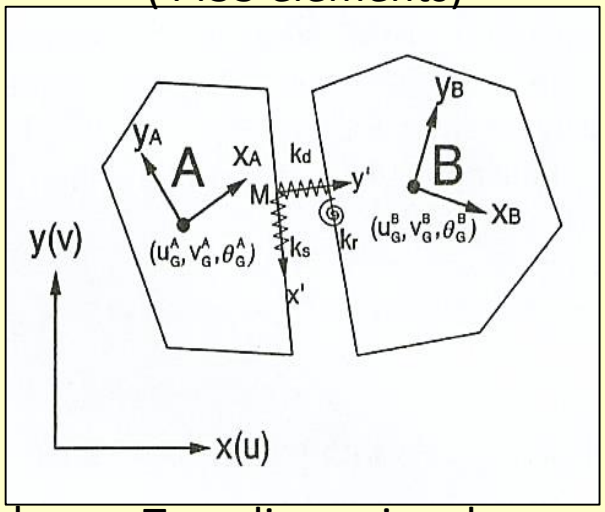

Two-dimensional polygonal RBSM

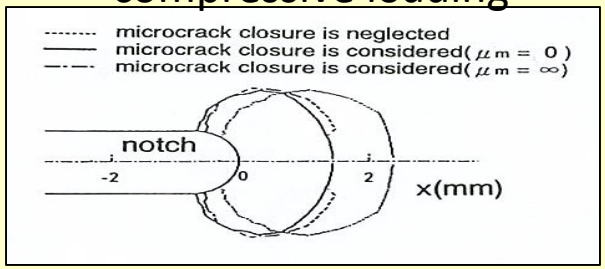

Distribution of microcrack density

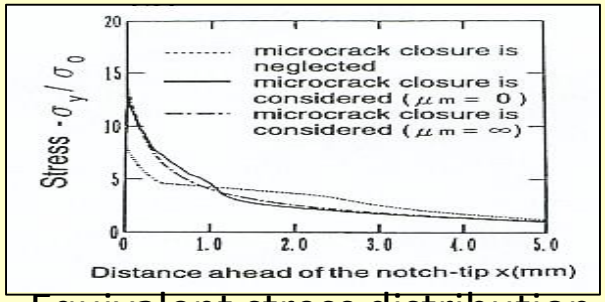

Equivalent stress distribution near the notch-tip

マイクロクラッキング脆性固体の三次元メソ解析と損傷力学モデルの改良 [26.都井・清末1993]

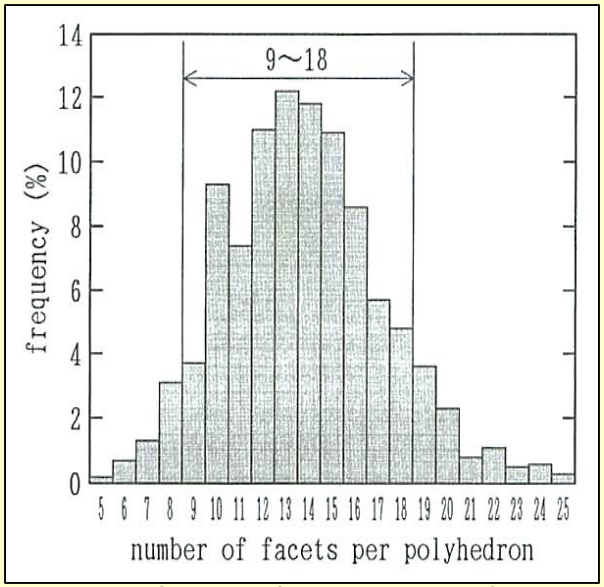

Three-dimensional polycrystalline model

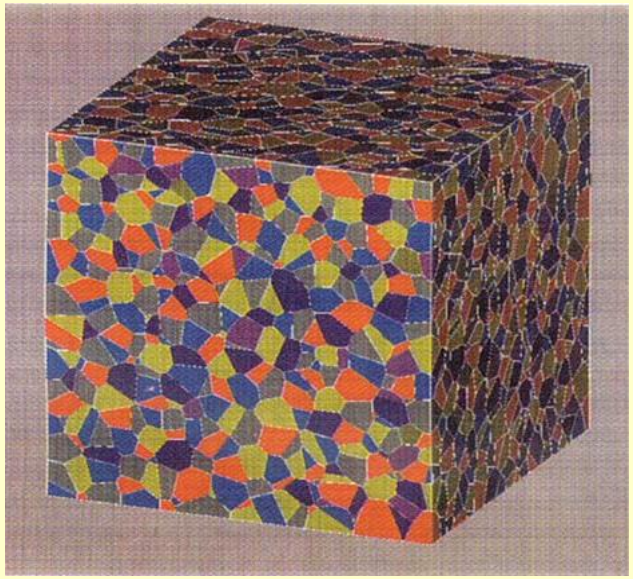

Statistics of three-dimensional Voronoi tessellation mesh

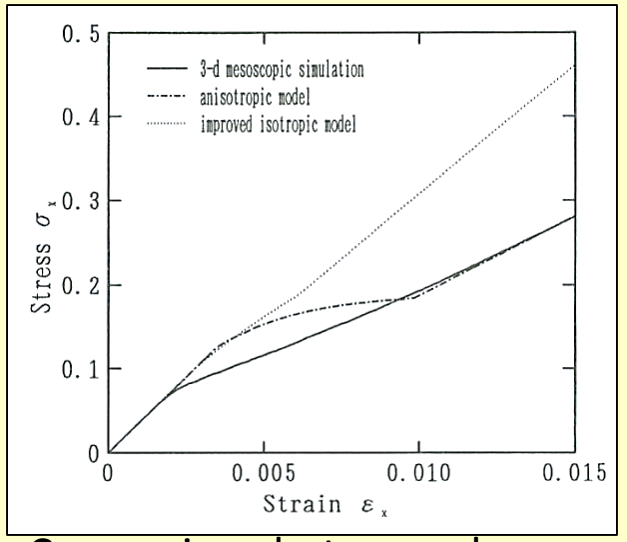

Comparison between damage mechanics models and 3D mesoscopic simulation under uniaxial tension

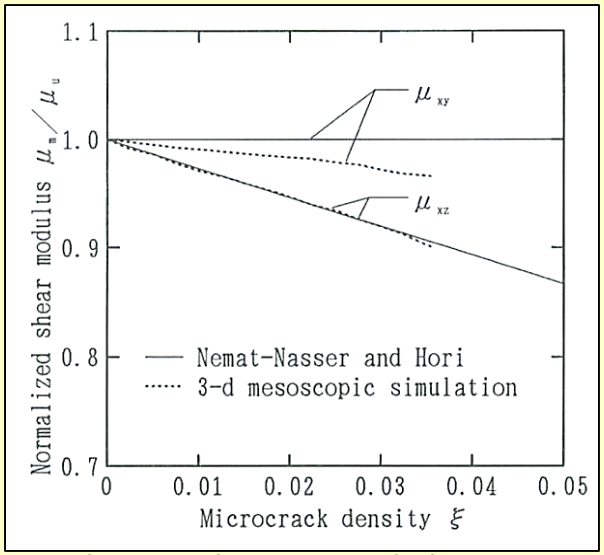

Elastic shear modulus vs. microcrack density under shear

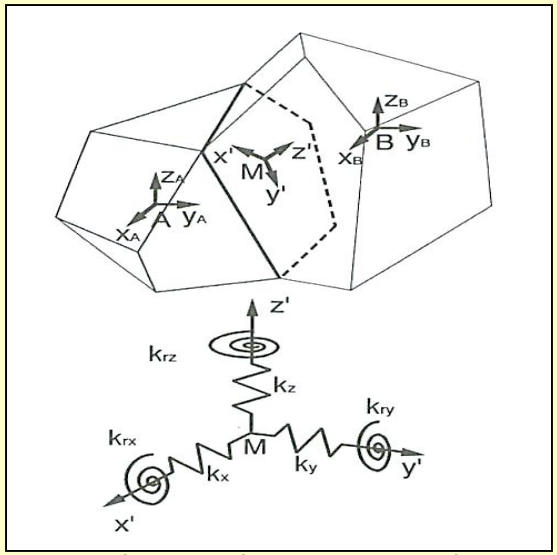

Three-dimensional mesoscopic model

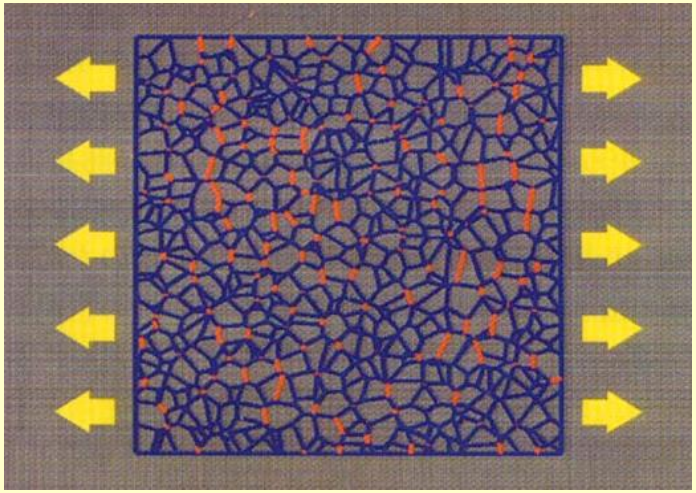

Microcracking pattern under uniaxial tension

変態塑性インクルージョンを含む二相材料の二次元メソ解析 [27.李廷権・都井1998]

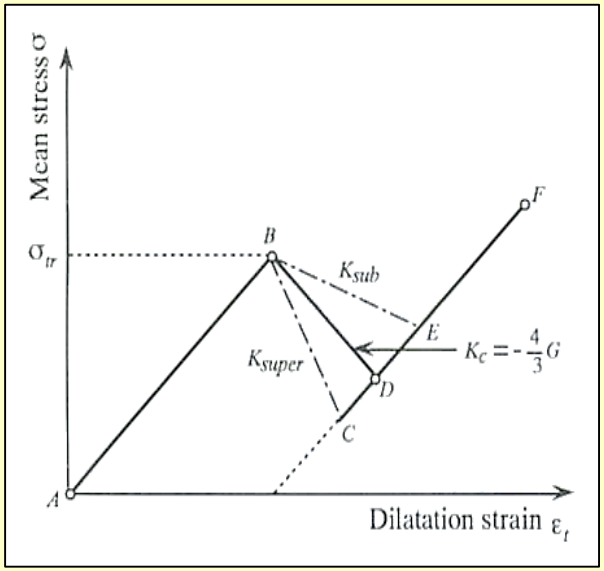

Schematic stress-strain relationship for the transformation plasticity behavior

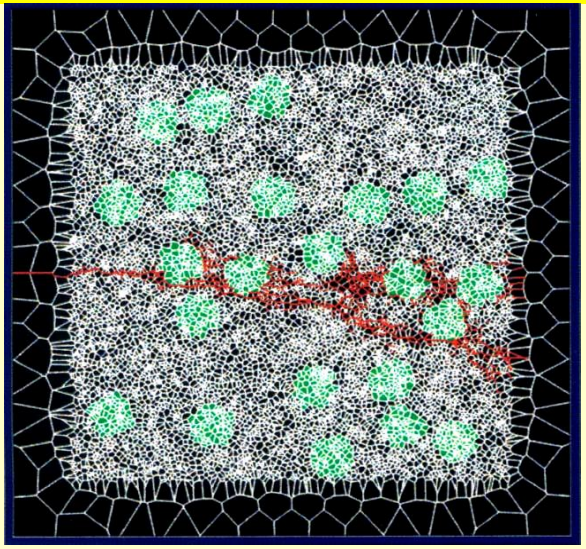

Crack propagation with transformation for the case of r_i=0.1r, A_i=16%

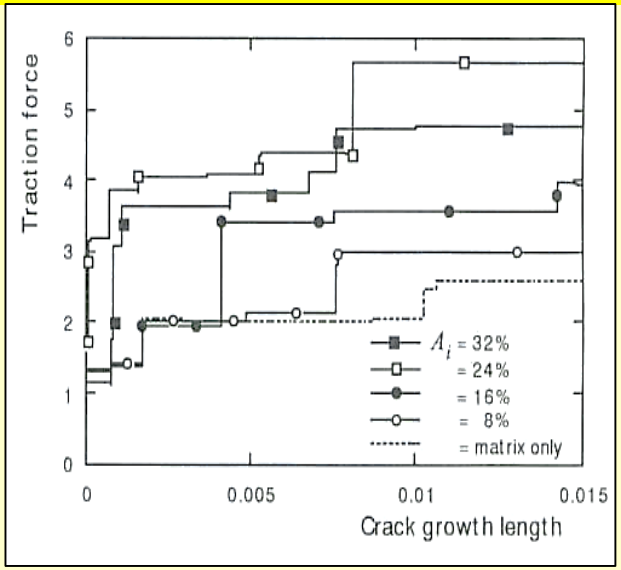

R-curves : Effect of area fraction with transformation for the case of r_i=0.1r, A_i=16%

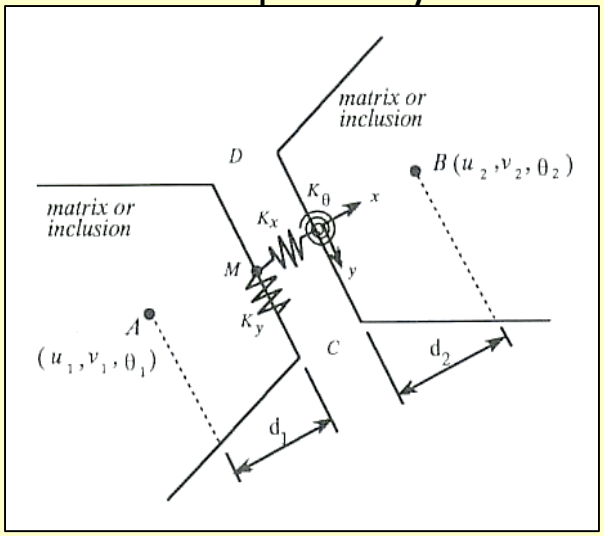

Two-dimensional mesomechanics model

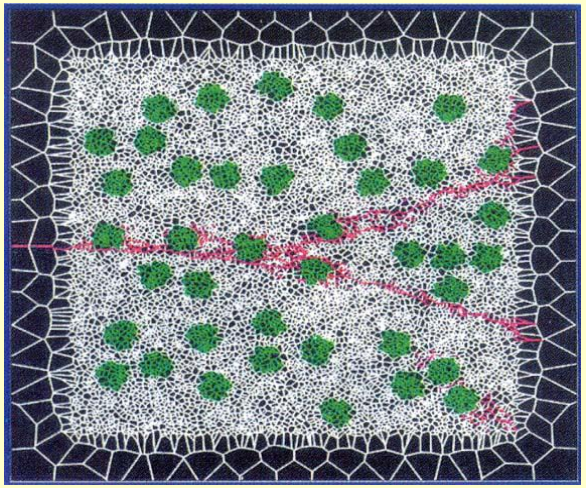

Crack propagation with transformation for the case of r_i=0.075r, A_i=16%

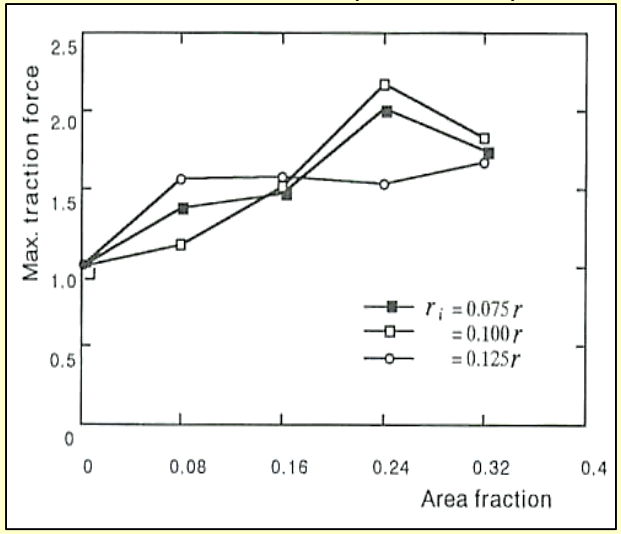

Effect of inclusion size with transformation

溶融亜鉛めっき時の構造部材の三次元損傷解析 [28.都井・李帝明2000]

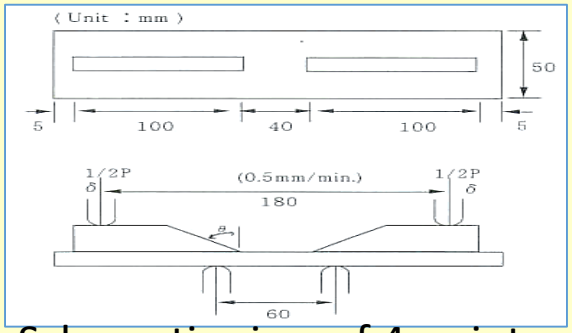

Schematic view of 4-point bending test in molten zinc

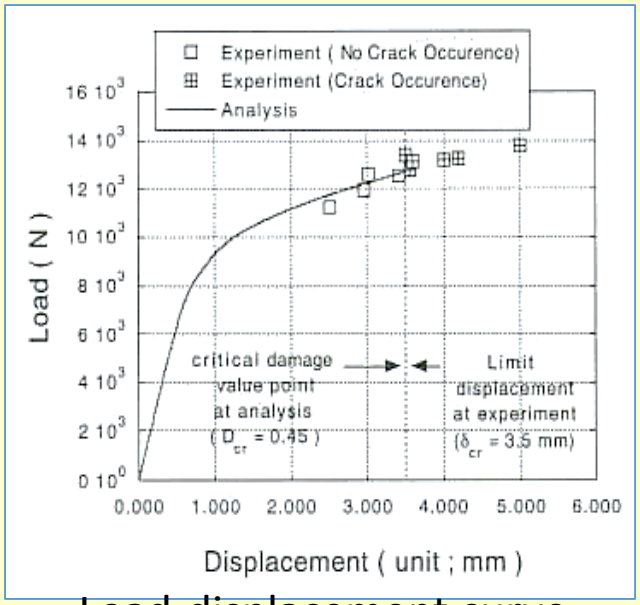

Load-displacement curve for bending test

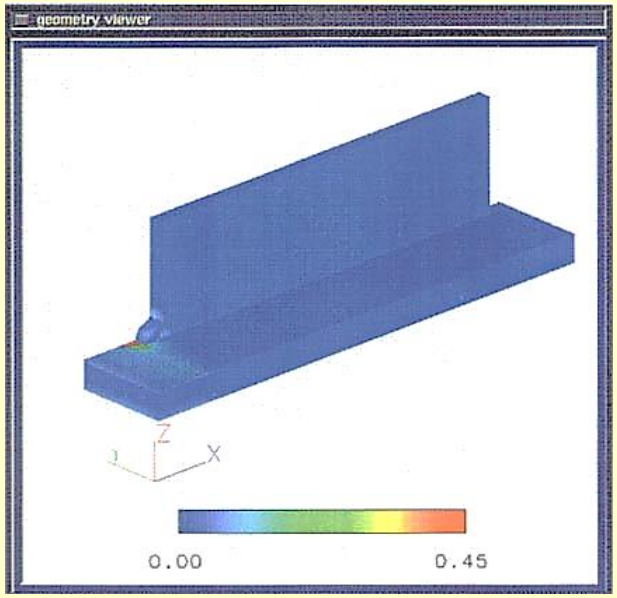

Distribution of damage (*t*=425s)

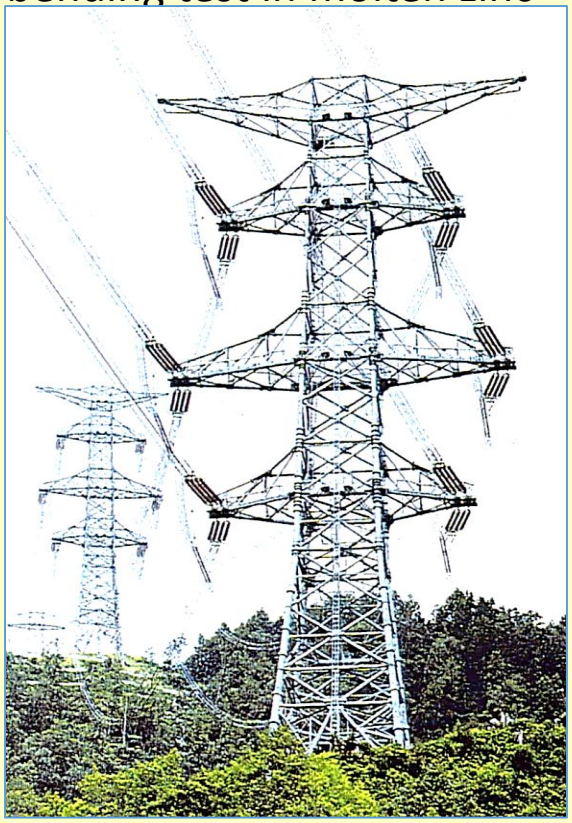

Pylon

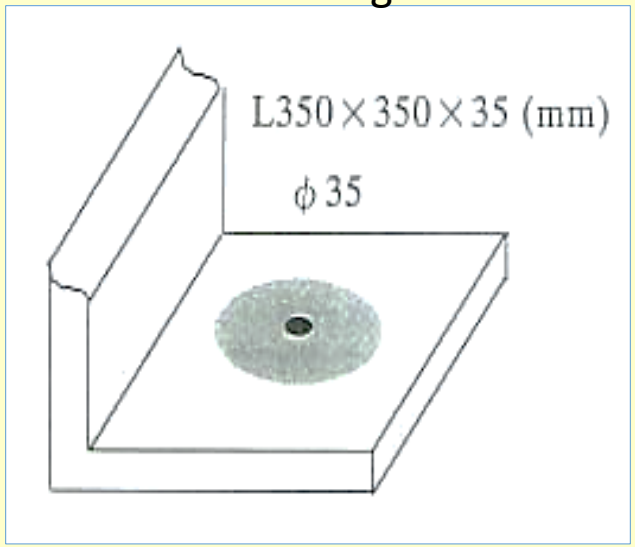

L-shaped steel pylon member with a bolt hole

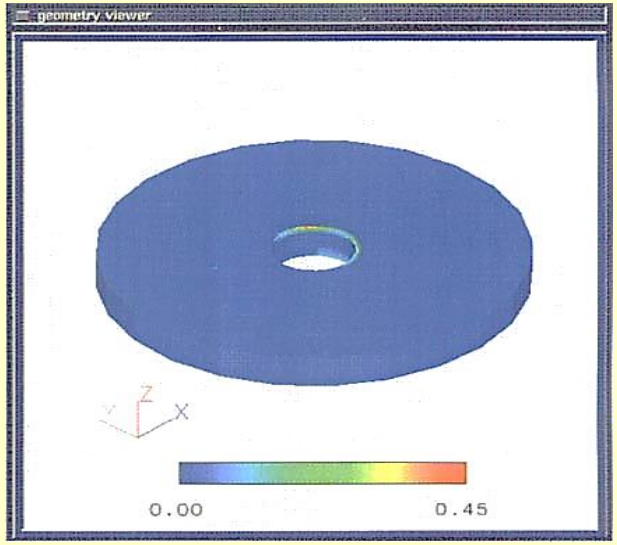

Distribution of damage (Mesh C)

鉄道レールの疲労損傷問題に対する計算力学的アプローチ [29.都井・李帝明・岩渕・森本・森2001]

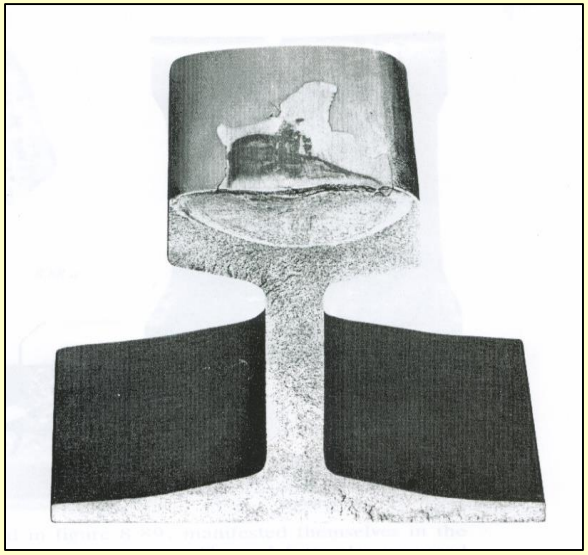

Fracture due to shelling

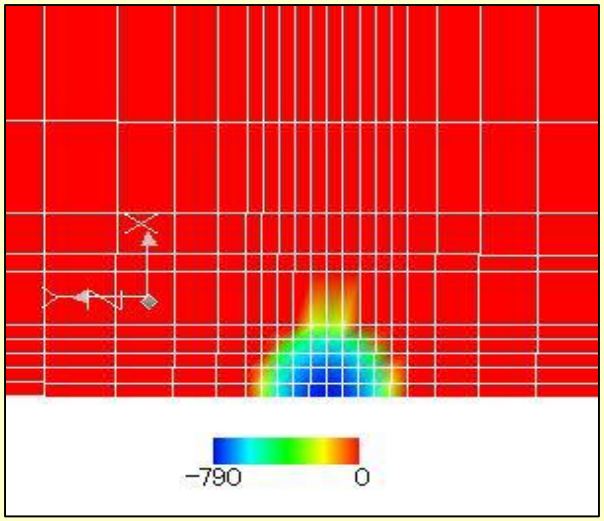

Distribution of normal load(Z-direction) calculated by Kalker's contact theory

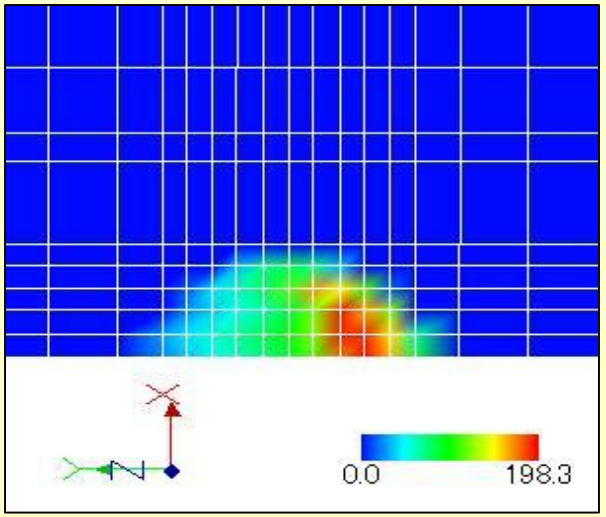

Distribution of tangential load(Y-direction) calculated by Kalker's contact theory

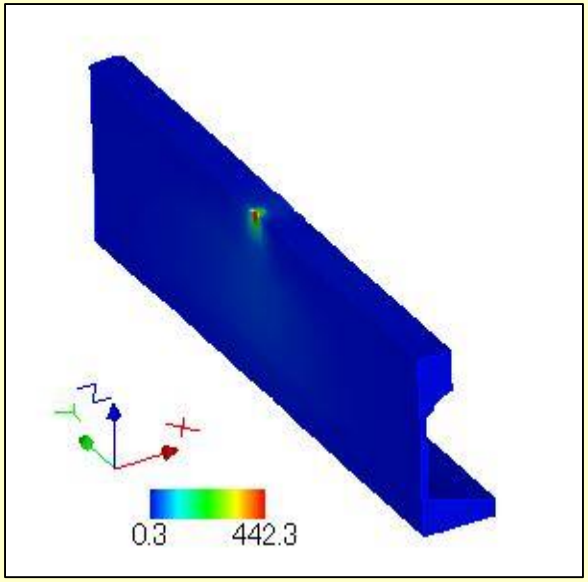

Distribution of equivalent stress (MPa)

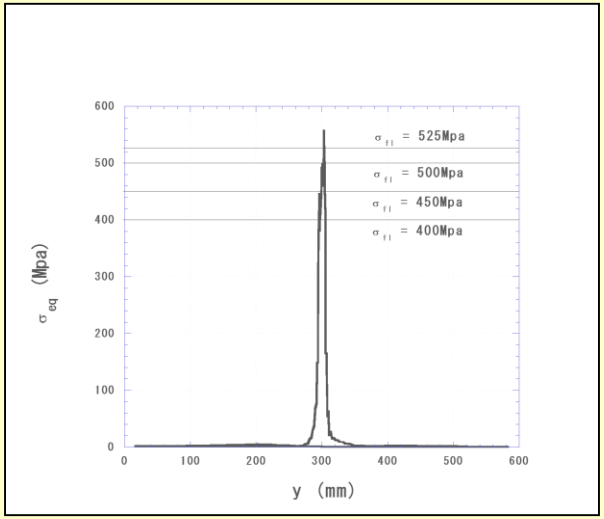

Equivalent stress distribution at the rail surface

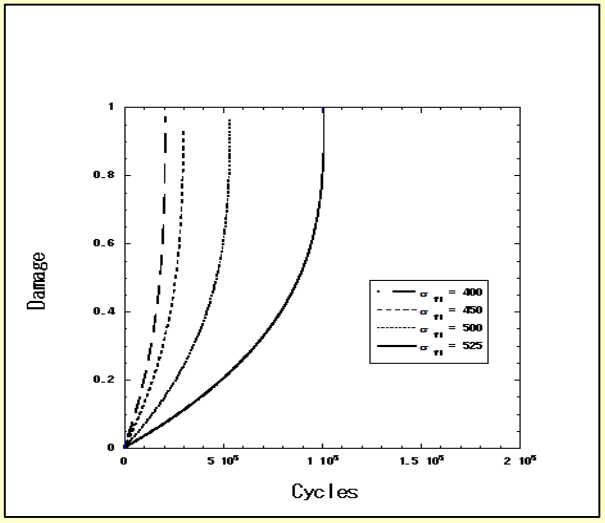

Damage evolution by the locally-coupled analysis

ズームイン方式による材料破壊問題のマルチスケール解析システムの開発
[30.都井・李廷権・李帝明・渡辺・酒井・顧・源2001]

Macroscale

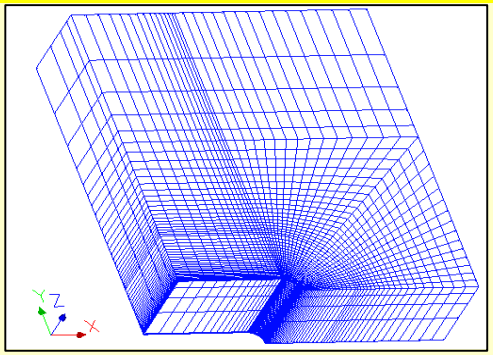

Finite element model for a notched specimen

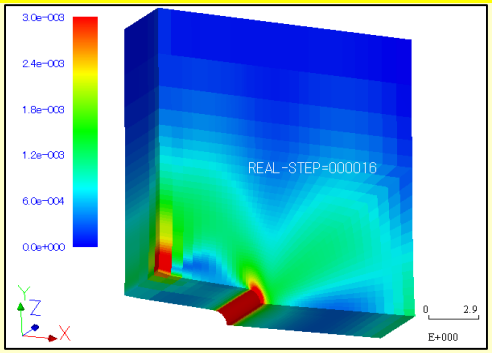

Deformation and equivalent strain

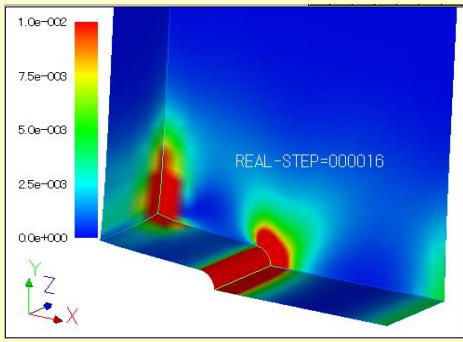

Damage distribution near the notch

Mesoscale

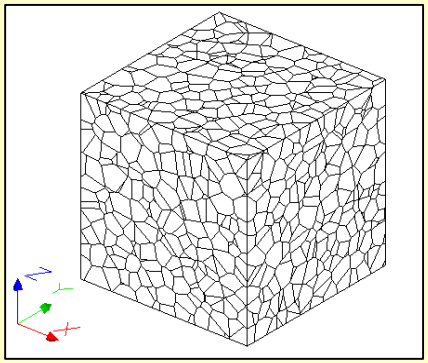

3-d polycrystalline model

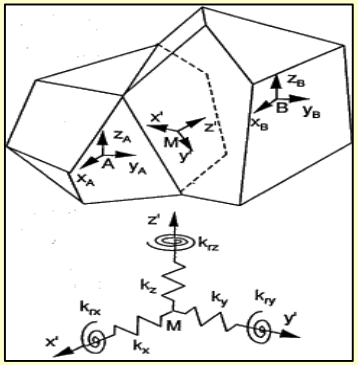

3-d mesomechanics model

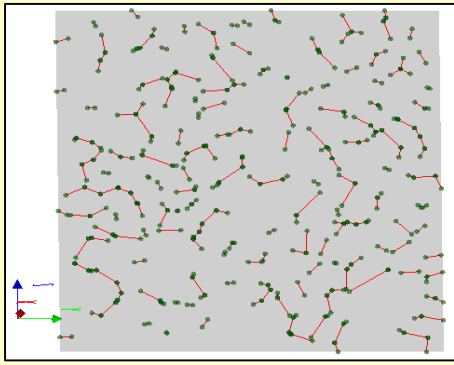

Microcrack distribution

Microscale

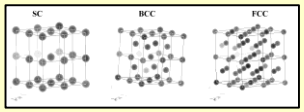

Molecular dynamics model

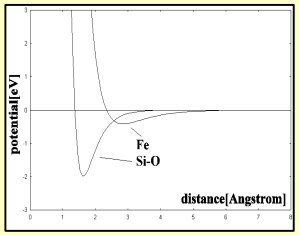

Potential curves

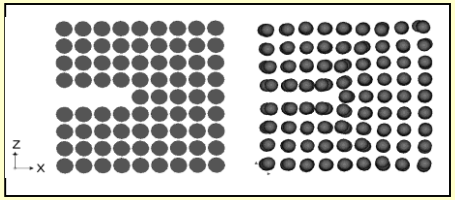

Initial state

Equilibrium state

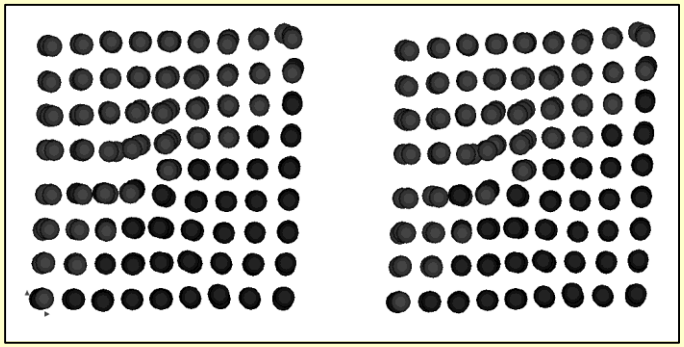

Fe-potential

Si-O potential

Deformation of fcc with initial defects

損傷力学モデルによる金属材料の力学特性の同定と予測［31.都井・広瀬2003］

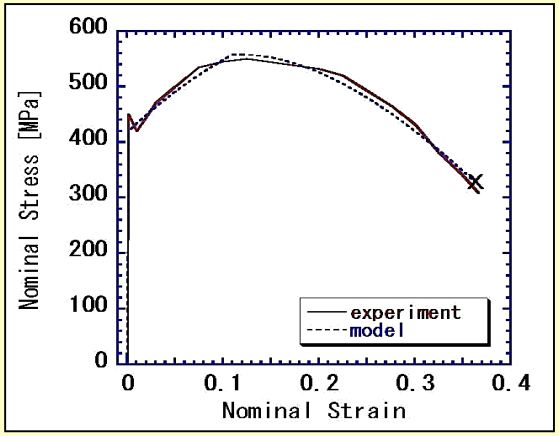

Quasi-static stress-stain curves of SM490A [*Itabashi*, 2001]

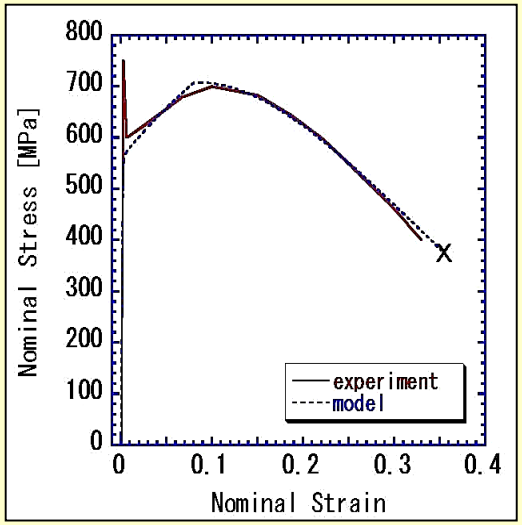

Dynamic stress-strain curves of SM490A [*Itabashi*, 2001]

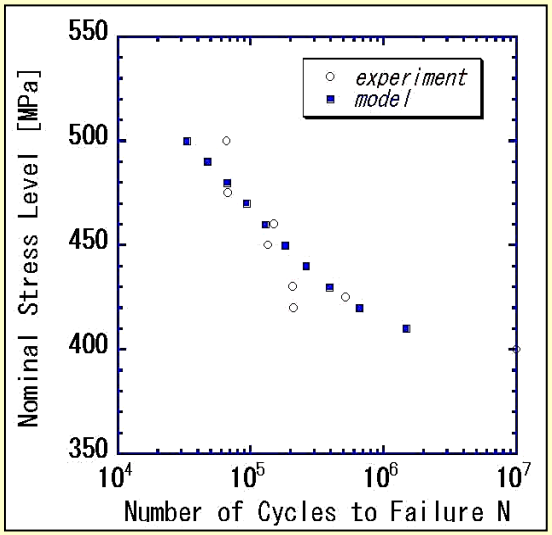

S-N curves for SM490A [*Itabashi*, 2001]

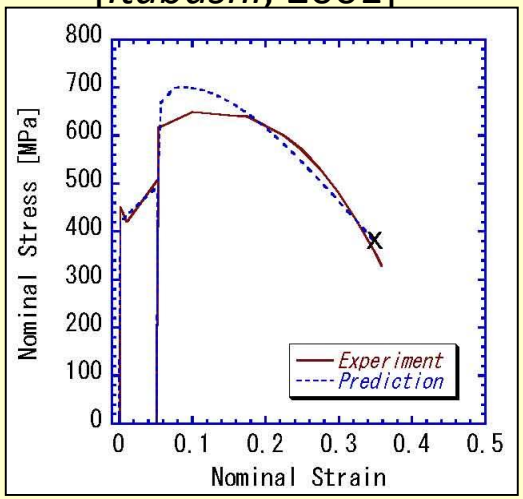

Dynamic stress-strain curve of pre-strained SM490A

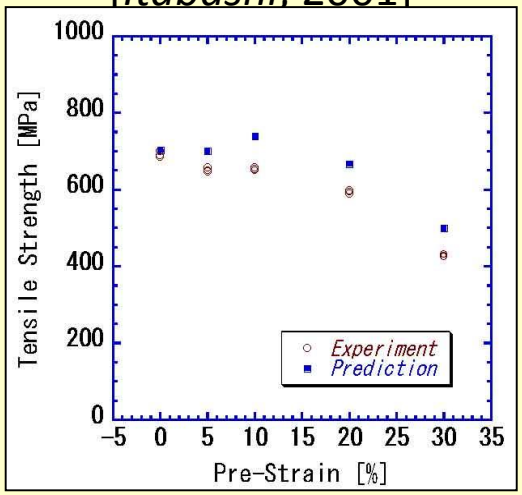

Tensile strength versus pre-strains for SM490A

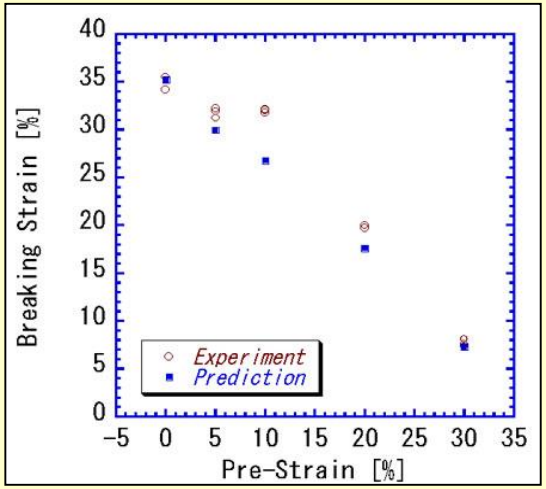

Breaking strains versus pre-strains for SM490A

損傷力学モデルに基づく数値材料試験法の疲労寿命予測への適用 [32.都井・広瀬・岩渕2004]

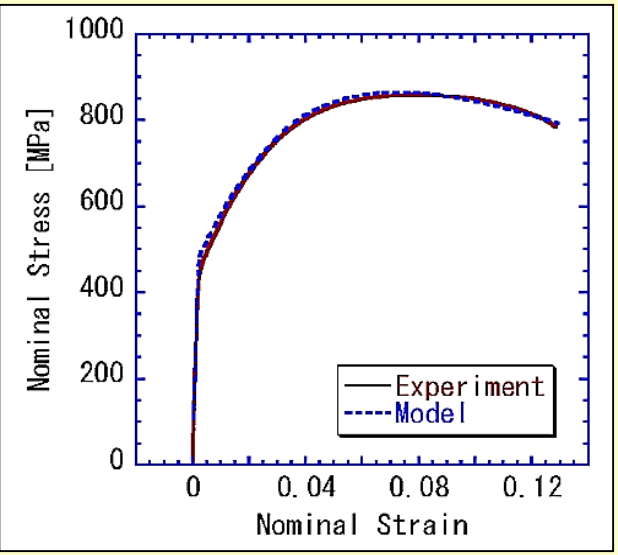

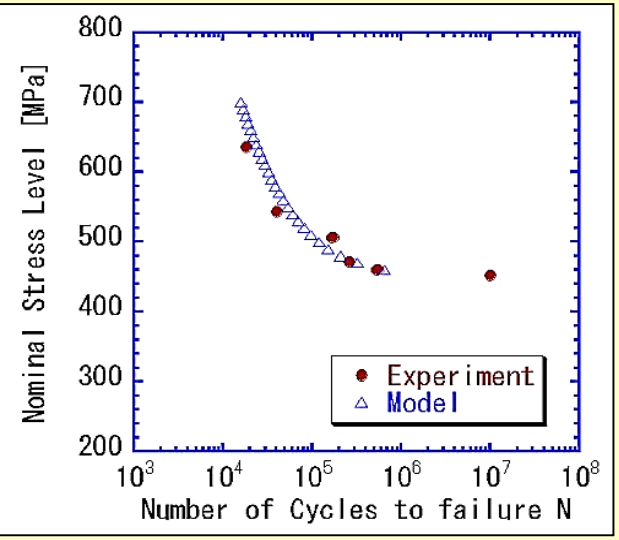

Results of material tests and model identification for steel

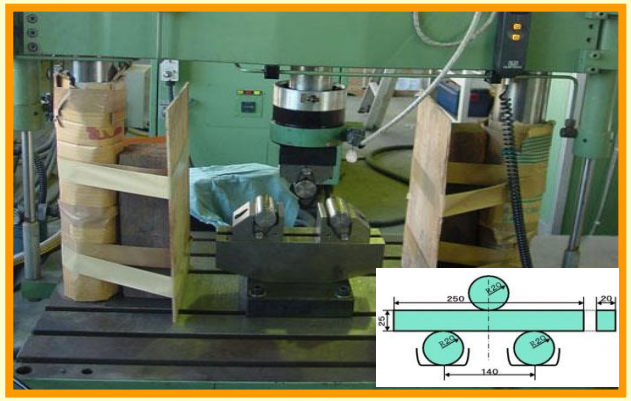

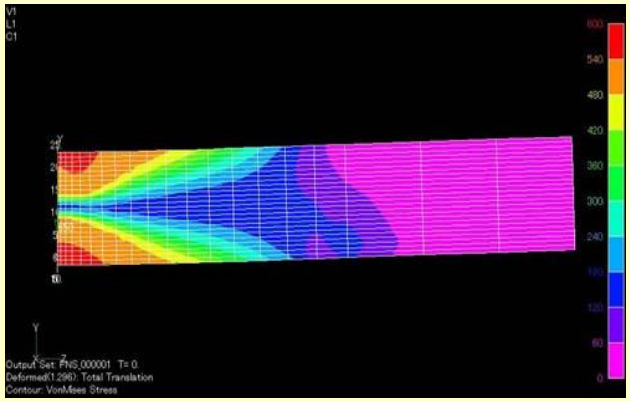

Equivalent stress distribution

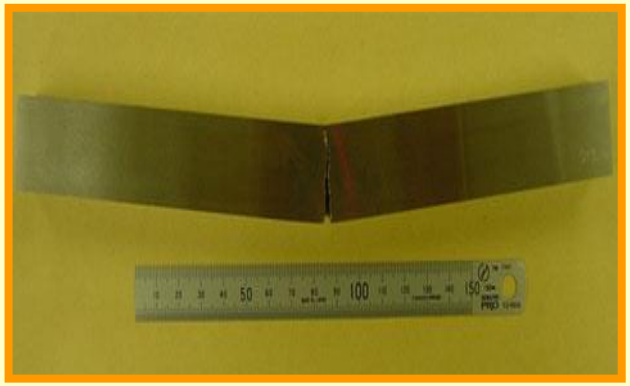

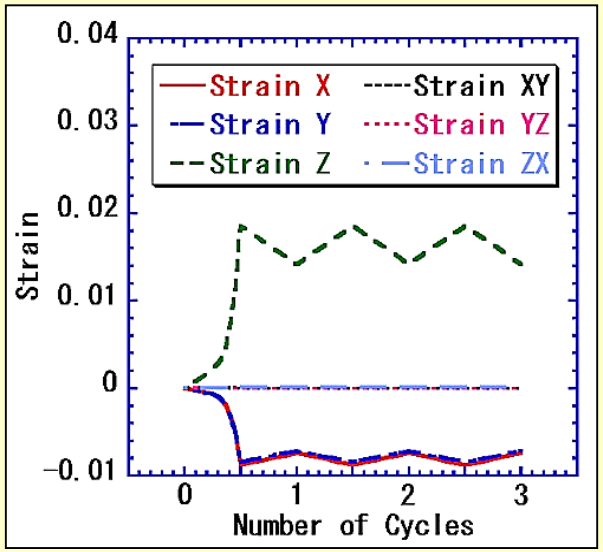

Strain histories

Experimental: 27000 cycles
Predicted: 32667 cycles

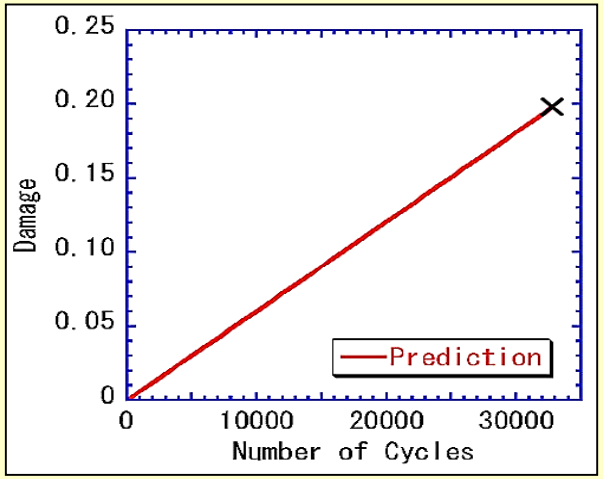

Predicted damage evolution

多数のボイドを含む固体の自然要素法によるメソスケール解析 [33.都井・姜2003]

Meshless methods:

Element-Free Galerkin Method (EFGM) [*Belytschko,* 1994]

Natural Element Method (NEM) [*Braun,* 1995]

from [*Sukumar,* 1998]

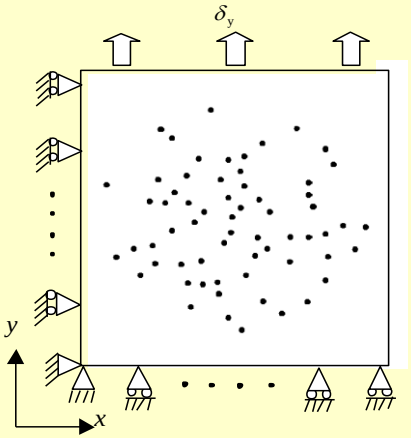

Boundary conditions

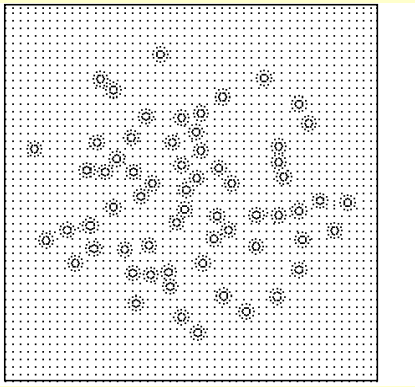

Nodal grid

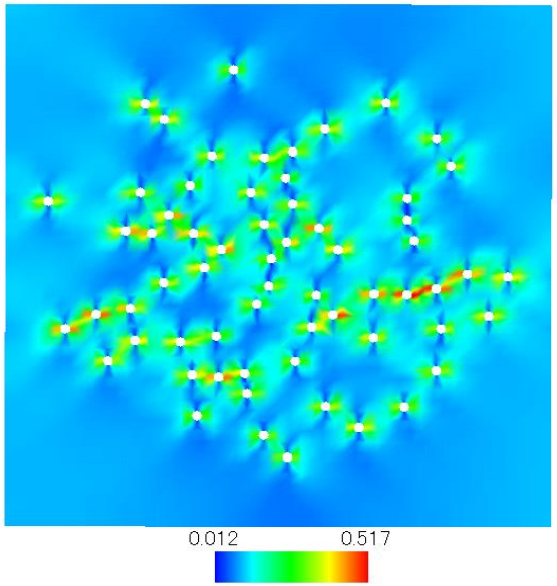

Distribution of equivalent strain for uniaxial tensile loading (at δy=7.935 mm)

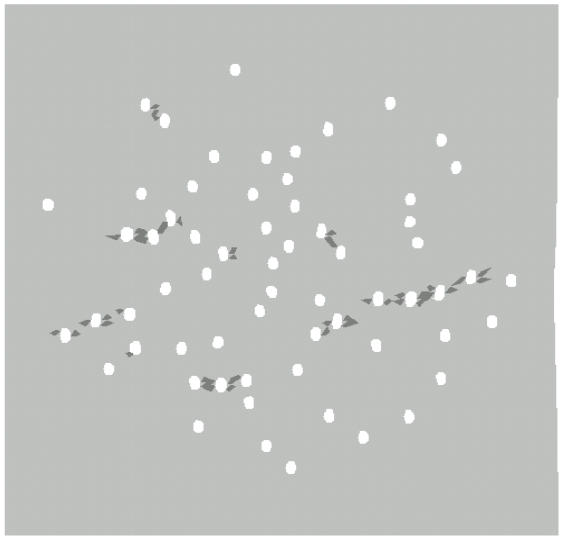

(a) at δy=8.895 mm

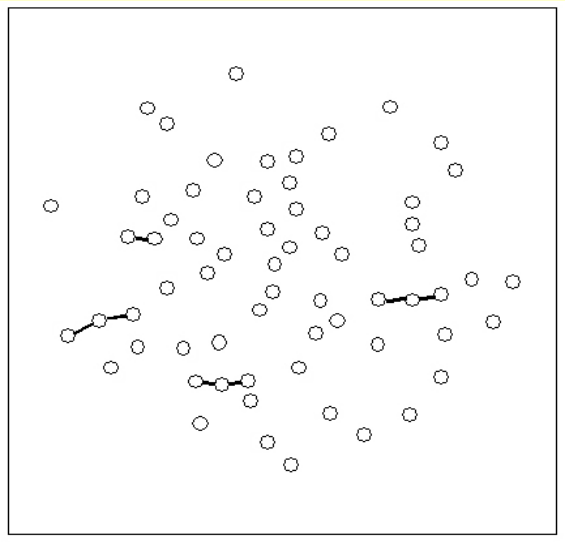

(b) Experiment [*Geltmacher,* 1996]

Deformation and void linking for uniaxial tensile loading

誘導加熱・熱弾粘塑性損傷・相変態の連成を考慮した三次元有限要素法による高周波焼入れ解析 [34.高垣・都井2005]

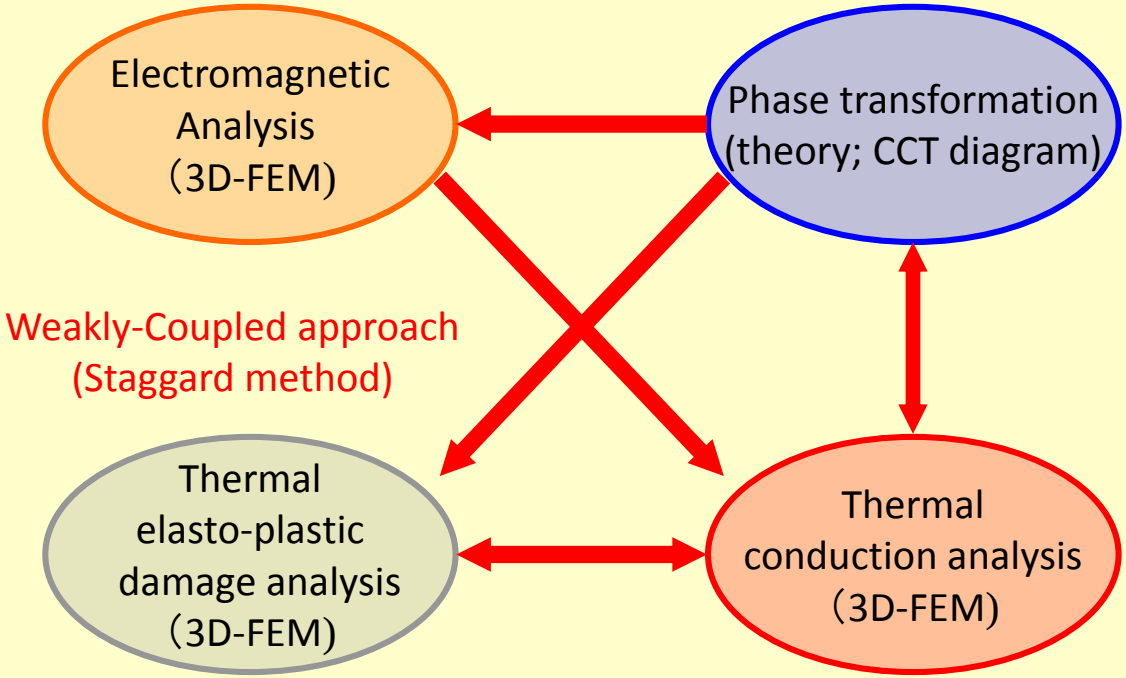

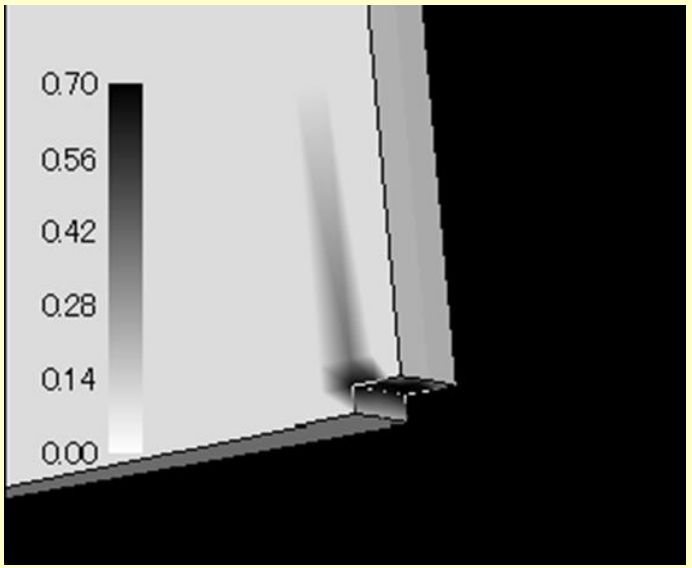

Damage distribution

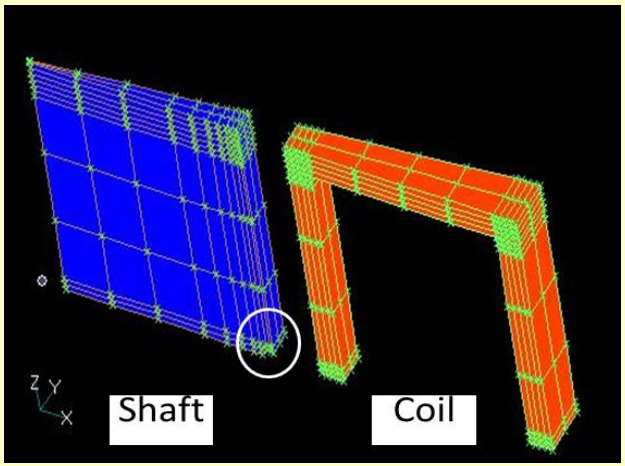

Notched bar and coil

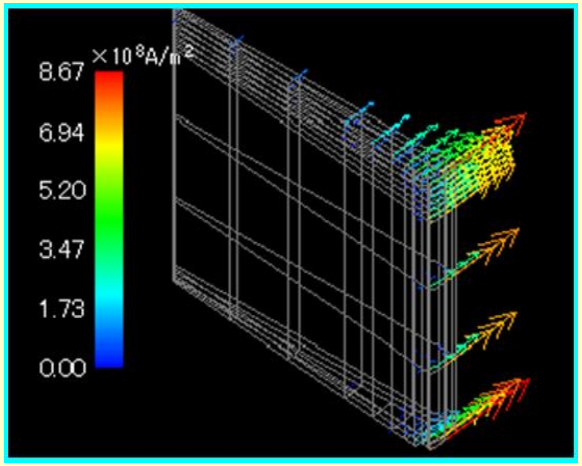

Eddy current density

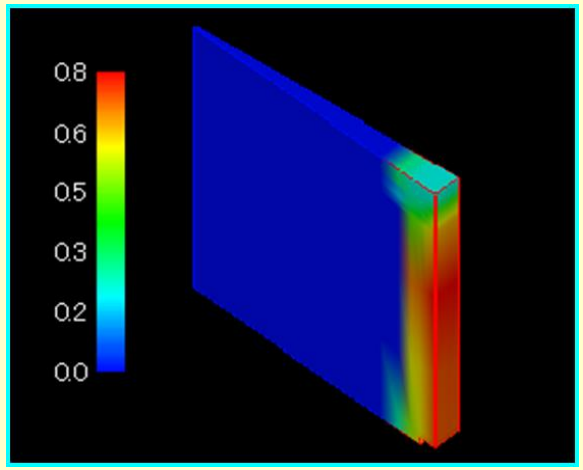

Martensite phase distribution

横衝撃を受ける多層塗膜の動的損傷挙動の有限要素解析① [35.都井・朴・中井・原2005]

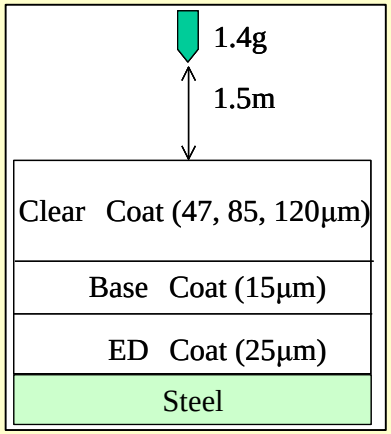

(a) STD model

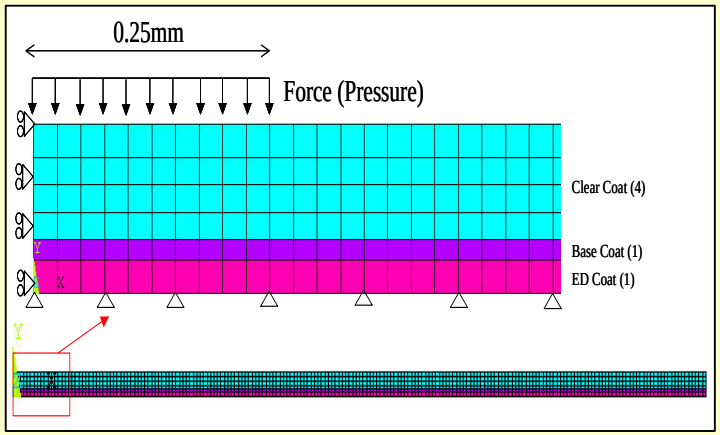

Finite element subdivision for STD model (CC-85μm)

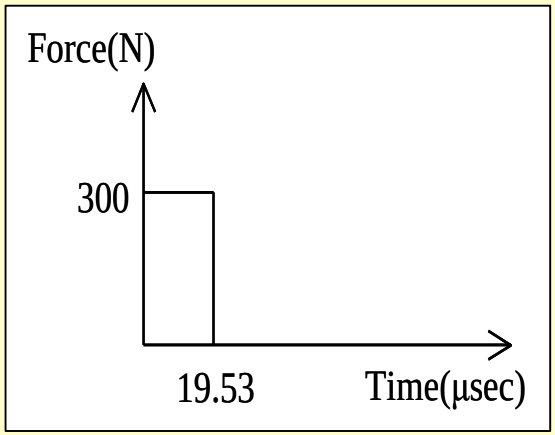

Loading condition for drop tests

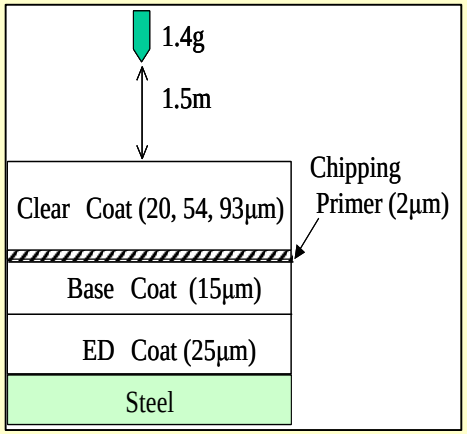

(b) CP model
Drop test for multi layer coatings

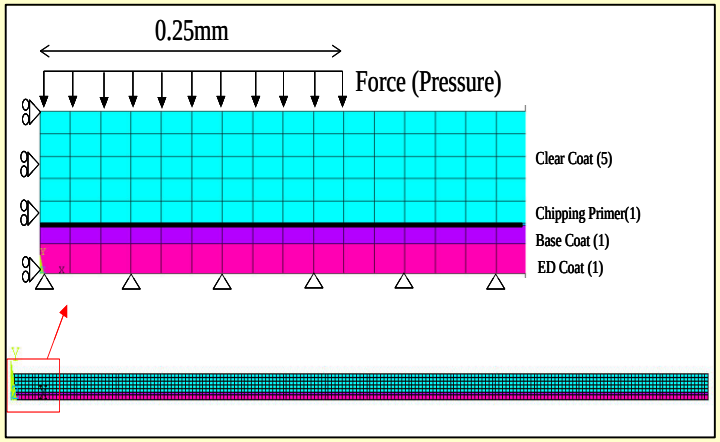

Finite element subdivision for CP model (CC-93μm)

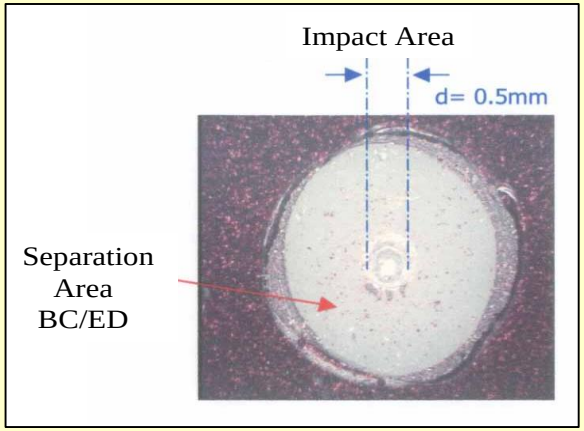

Fracture in drop tests

横衝撃を受ける多層塗膜の動的損傷挙動の有限要素解析② [35.都井・朴・中井・原2005]

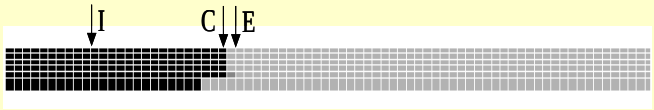

(a) Thickness (CC + BC) - 62μm

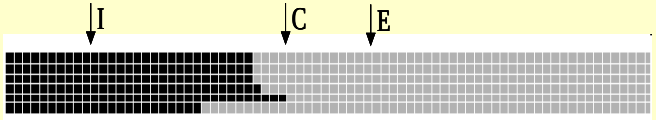

(b) Thickness (CC + BC) - 100μm

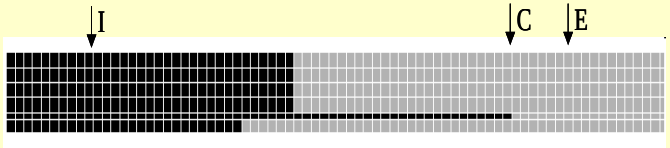

(c) Thickness (CC + BC) - 135μm

Damage distributions in STD models

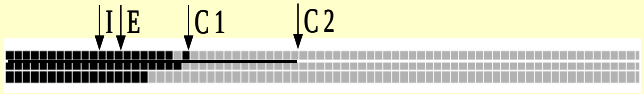

(a) Thickness (CC + CPr + BC) - 37μm

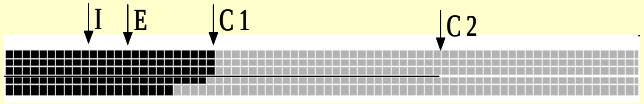

(b) Thickness (CC + CPr + BC) - 71μm

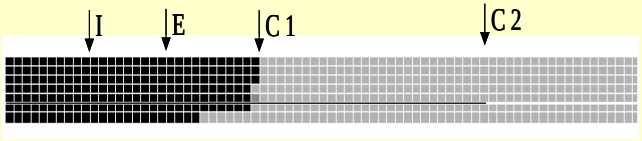

(c) Thickness (CC + CPr + BC) - 110μm

Damage distributions in CP models

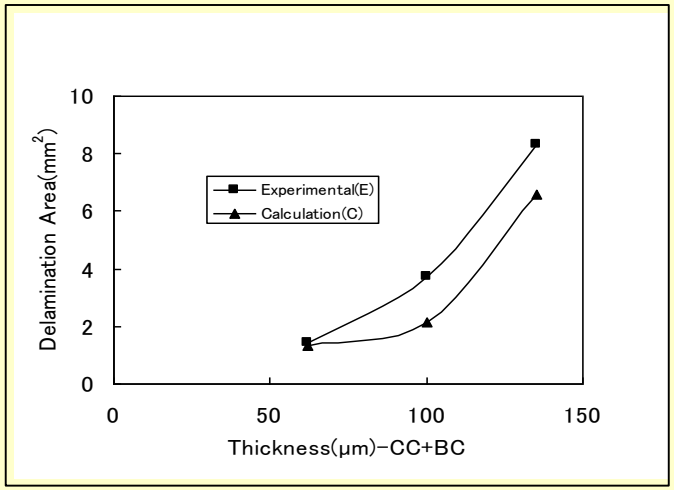

Delamination area in STD models

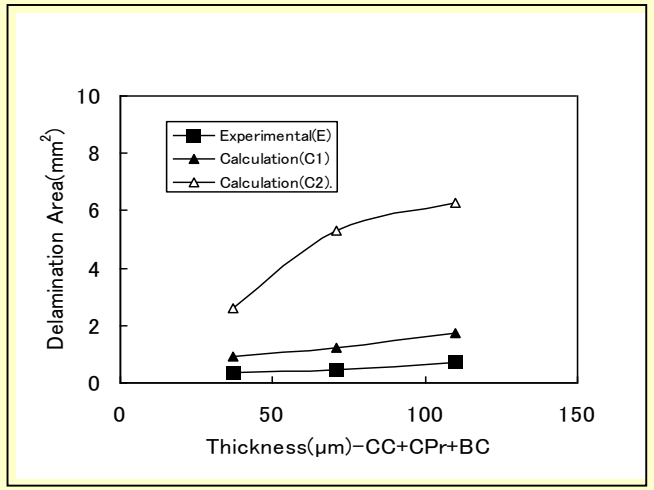

Delamination area in CP models

炭素繊維シートにより補強された脆性体構造要素の損傷破壊解析 [36.田中・都井・前田・酒井2006]

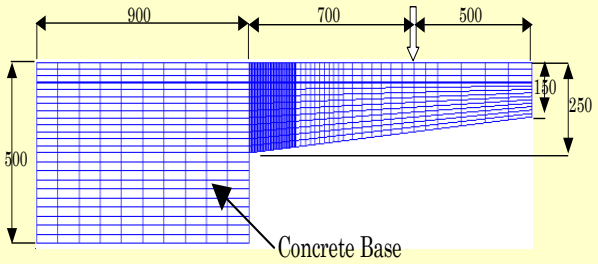

Drucker-Prager equivalent stress

$\sigma_e = \beta J_1 + (J_2')^{1/2}$

J_1 : 1st invariant of stress

J_2' : 2nd invariant of deviatoric stress

Strengthened part of bridge

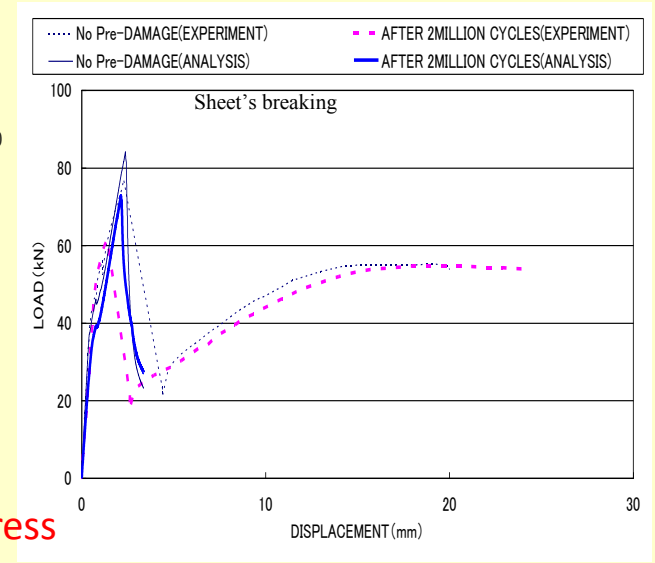

Load-displacement curves (with CF sheet)

Fracture (with CF sheet)

Experimental overview

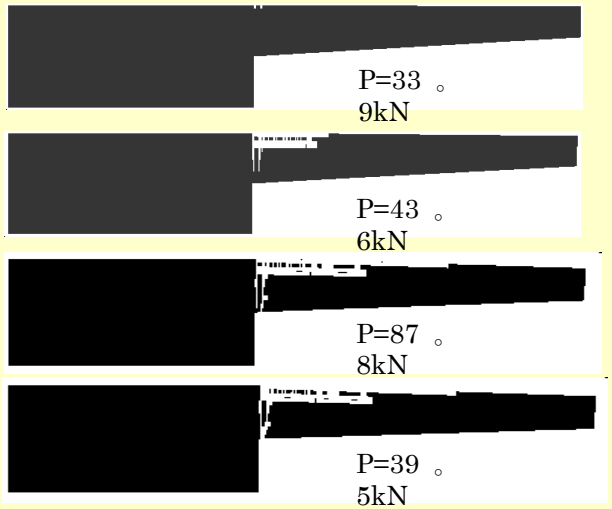

Damage distribution (with CF sheet)

Fracture (with CF sheet)

局所的破壊解析法を用いた熱疲労解析によるき裂進展挙動評価 [37.高垣・都井・浅山2006]

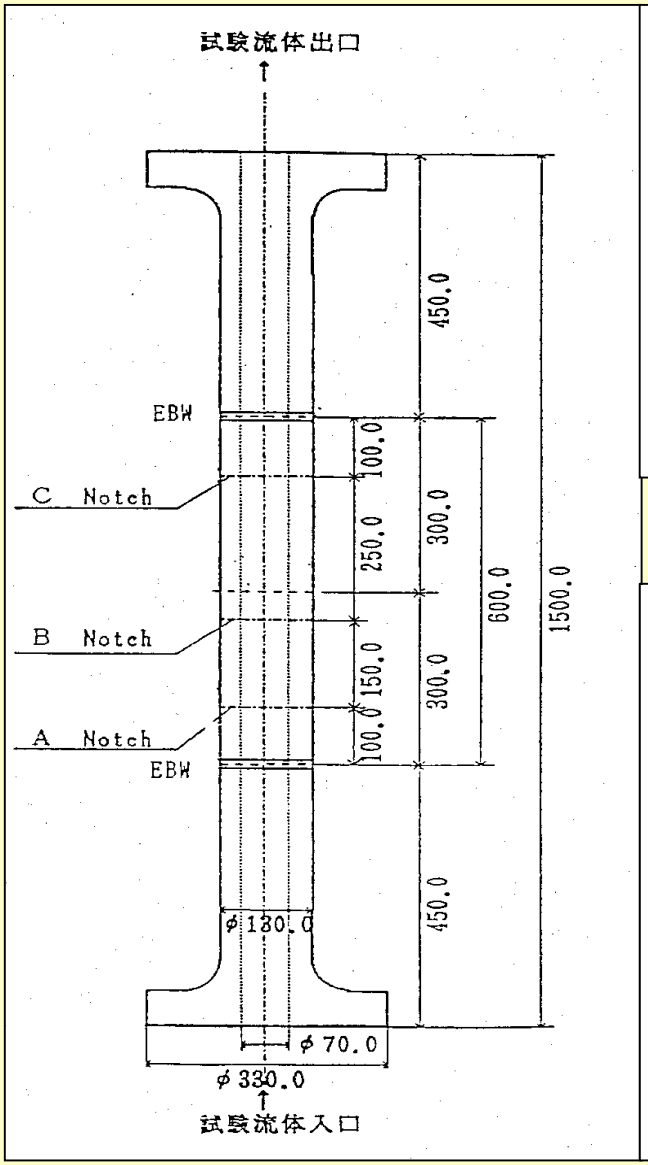

SUS304 cylinder under thermal cycle

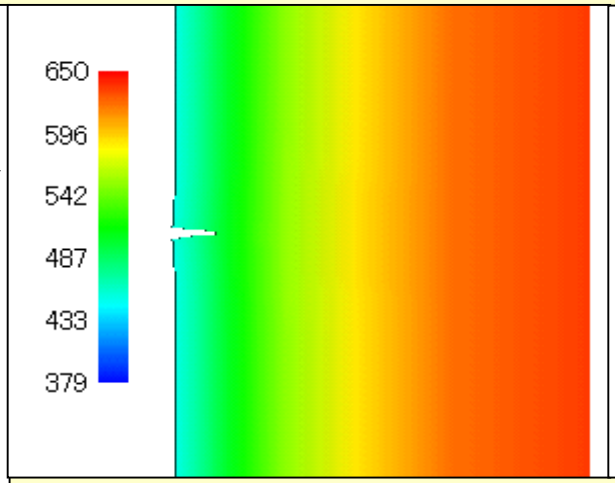

Temperature distribution at cooling

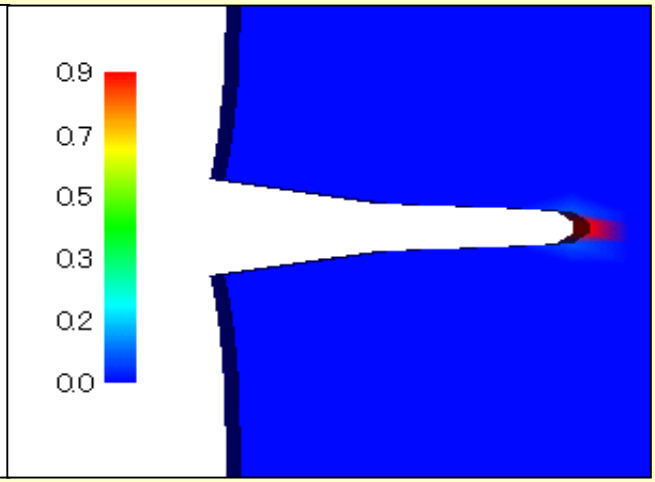

Damage distribution near C notch

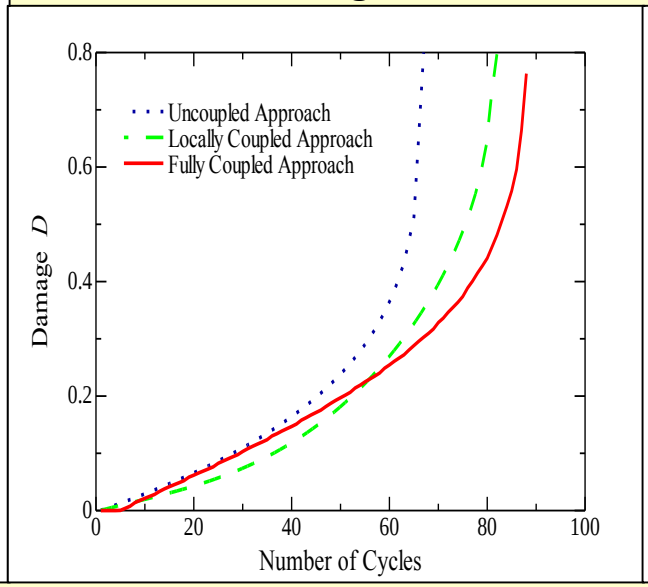

Damage history at C notch tip

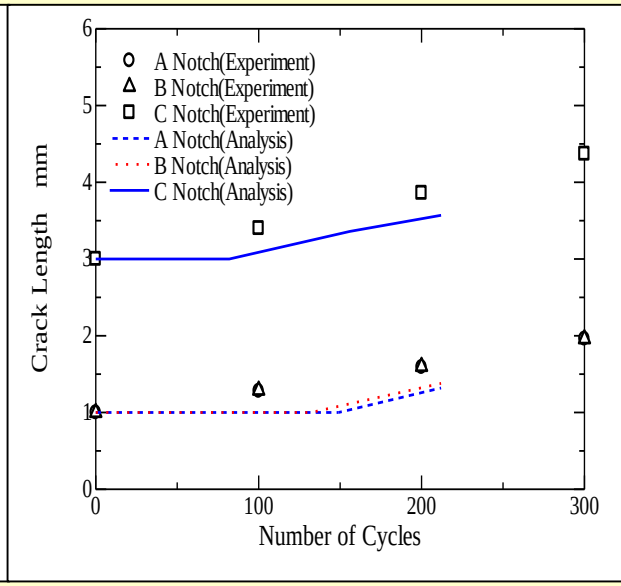

Crack propagation

金属接合の熱疲労寿命シミュレーション① [38.都井・広瀬2008a]

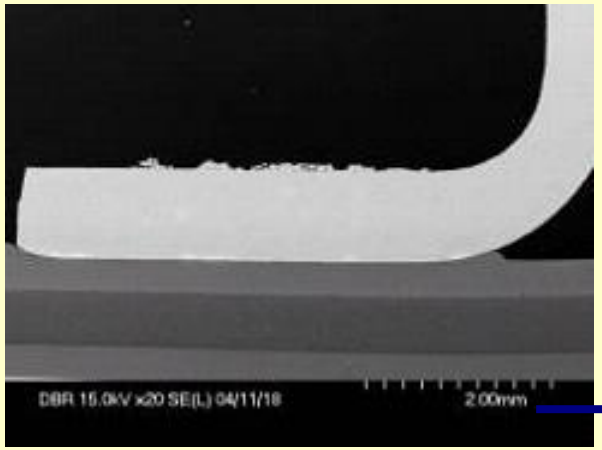

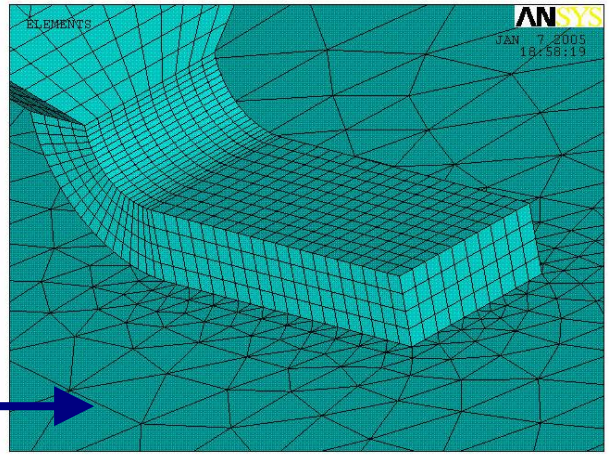

Conductor joint by vibration bonding

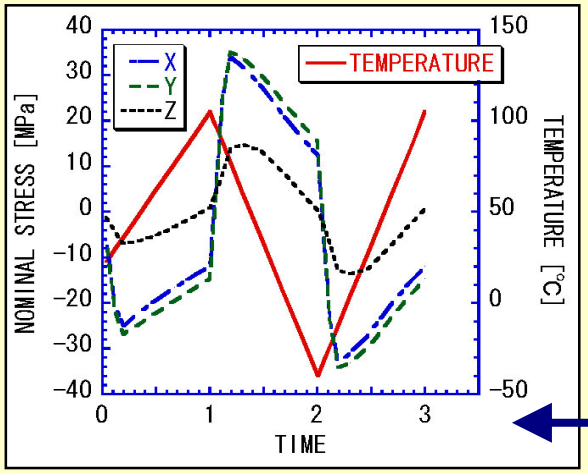

25 → 105 → -40 → 105℃

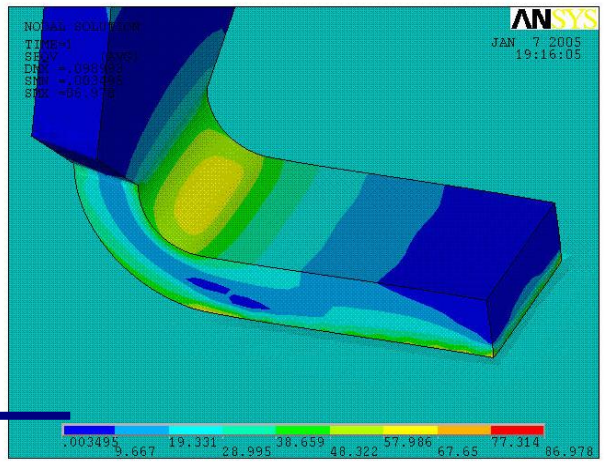

Cohesive fracture in aluminum under joint

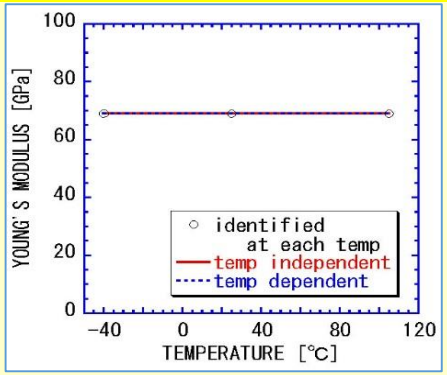

Young's modulus

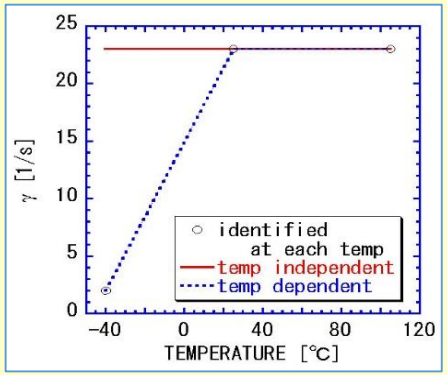

Viscous coefficient

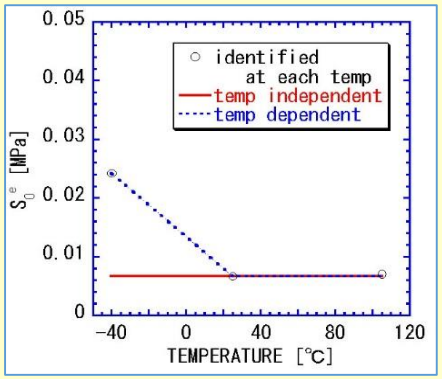

Damage parameter

金属接合の熱疲労寿命シミュレーション② [39.都井・広瀬2008b]

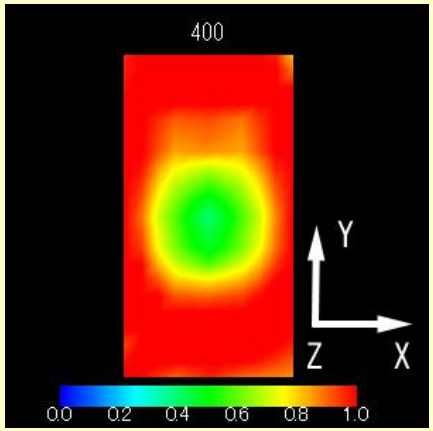

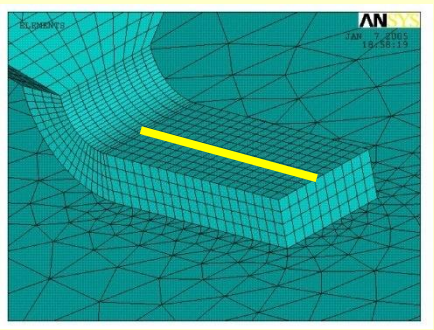

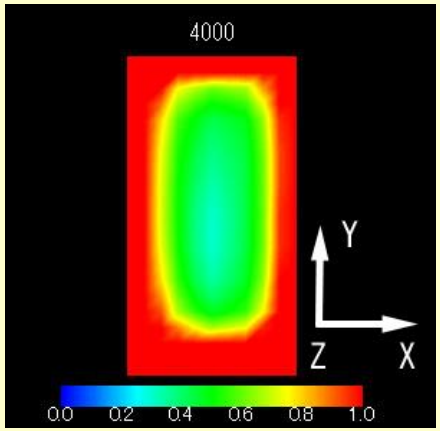

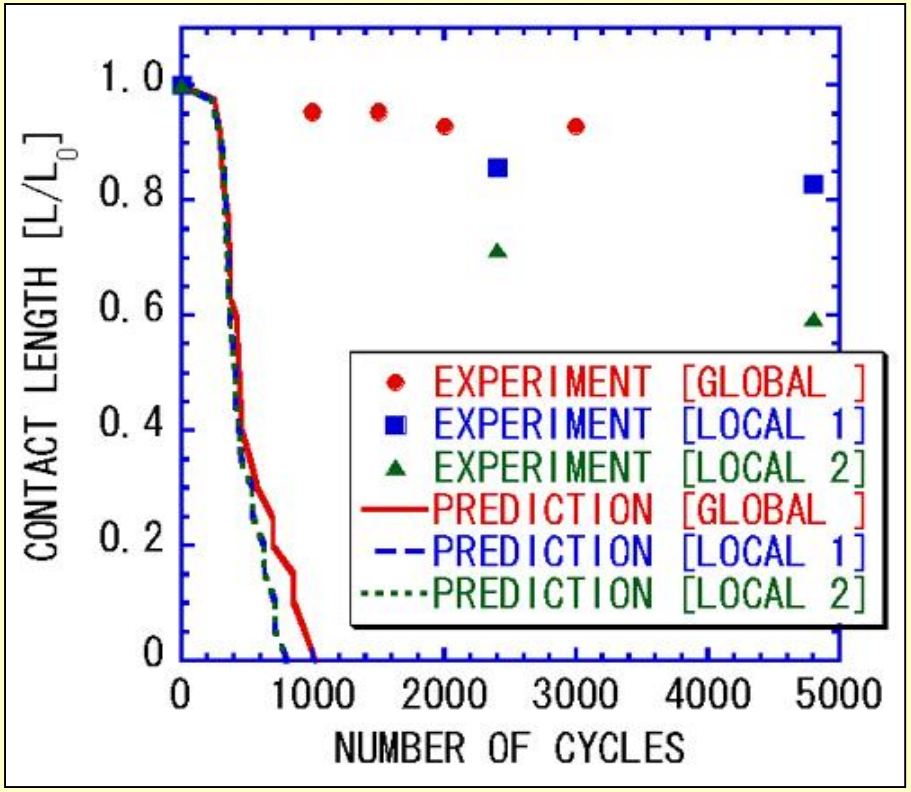

Temperature dependent, no stress reduction

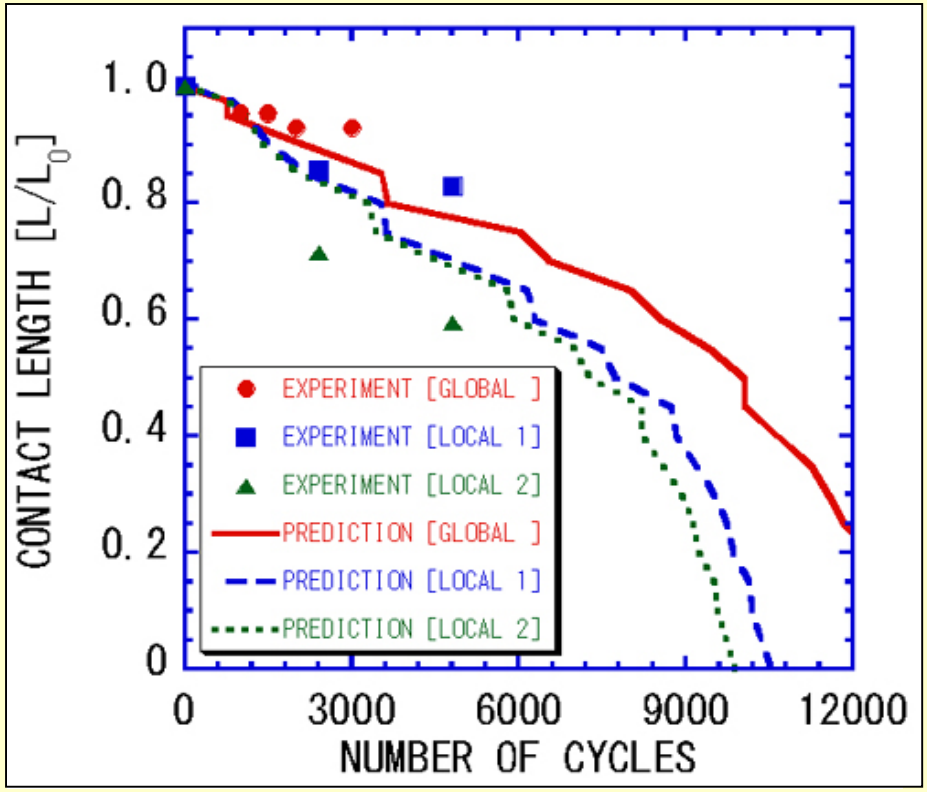

Temperature dependent, 10% stress reduction

クリープ損傷を受けた鋼材の自己修復過程のシミュレーション① [40.都井・広瀬2005]

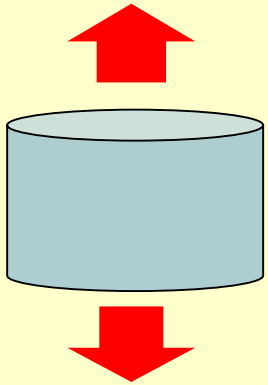

Creep by tension

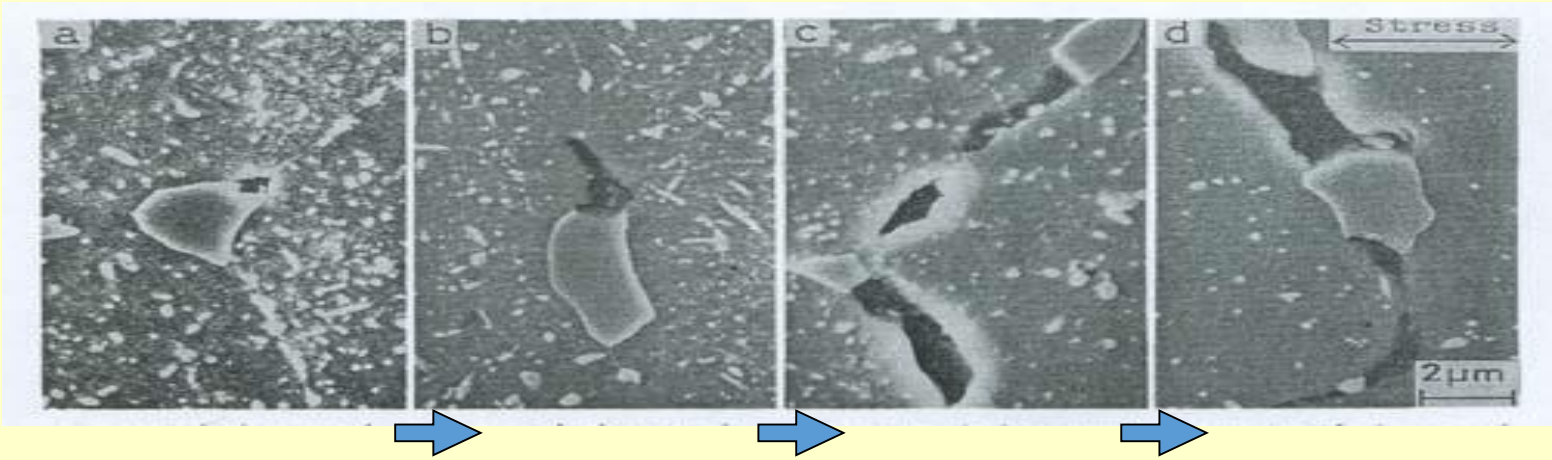

Growth of typical cavities observed in specimens crept in tension
[*Kyono,* 1993] [*Murata*, 1990]

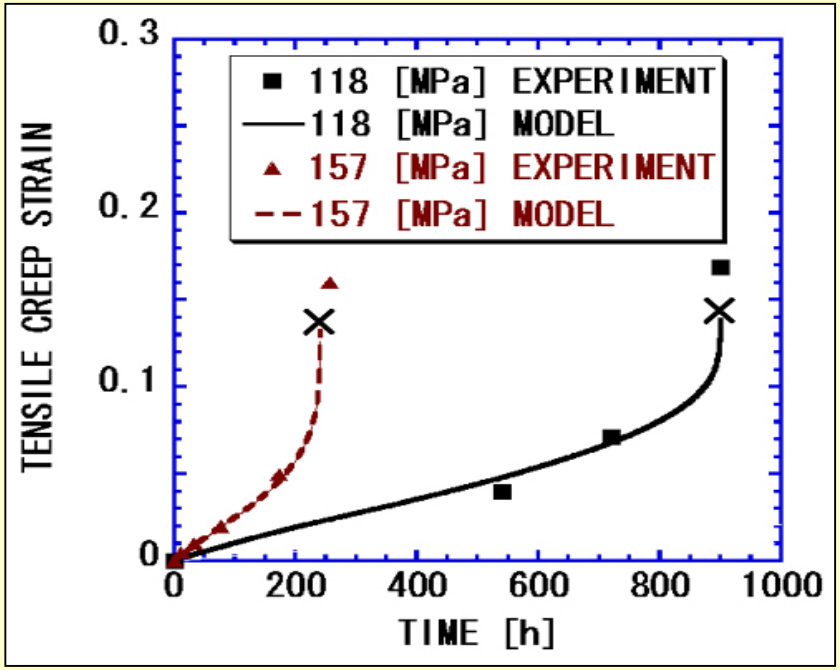

Tensile creep curves for SBV2 [*Kyono,* 1993]

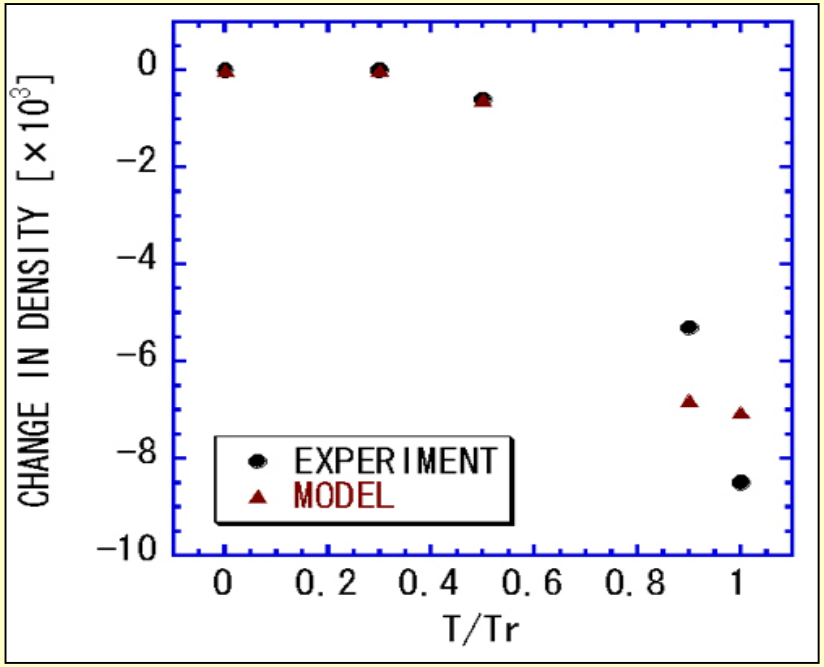

Change in density for [*Murata*, 1990]

クリープ損傷を受けた鋼材の自己修復過程のシミュレーション② [40.都井・広瀬2005]

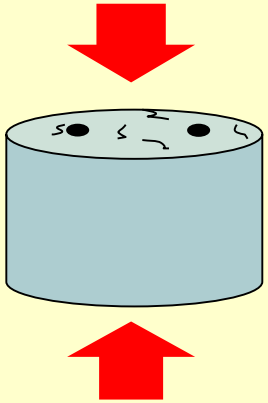

Sintering by compression

Decrease of typical cavities observed in specimens crept in compression [*Kyono,* 1993] [*Murata*, 1990]

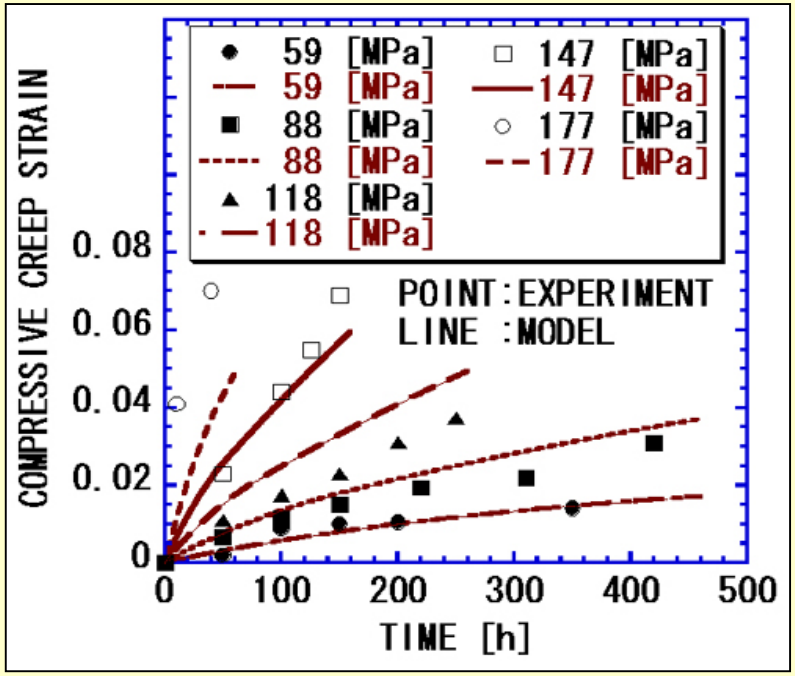

Compressive creep curves for SBV2 [*Kyono,* 1993]

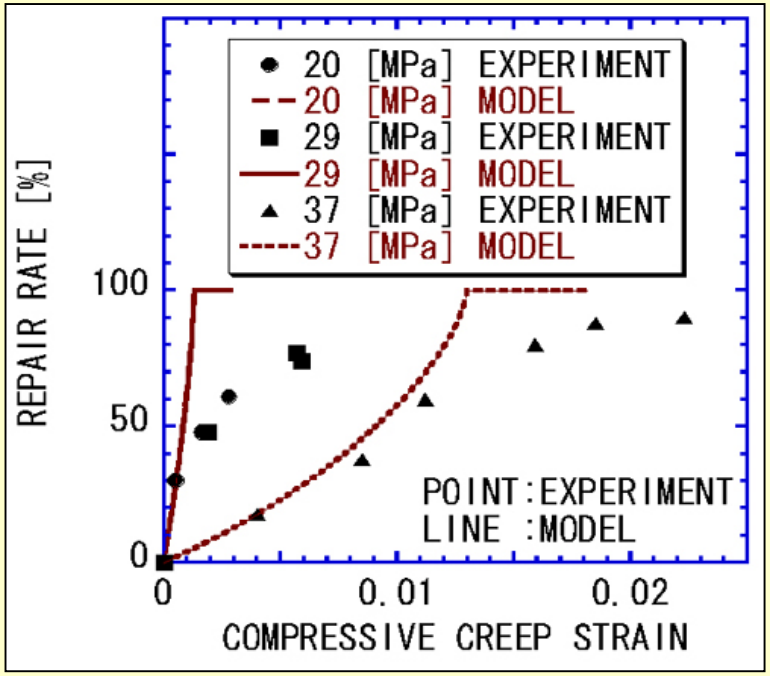

Repair rate for SUS316HTB [*Murata*, 1990]

溶射コーティングの損傷挙動のシミュレーション [41.都井・杉崎・栗栖・四阿・線2009]

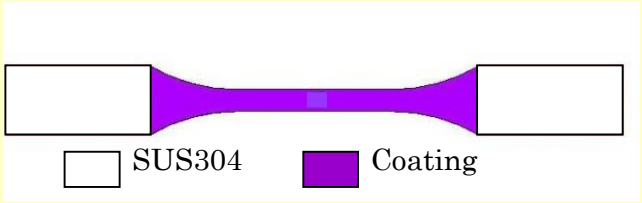

Material	Composition	Coating Method	Thickness
Cermet	40%-Carbide Cermet	HVOF (High Velocity Oxy-Fuel) Thermal Spraying	185 μm
	75%-Carbide Cermet		213 μm

Test specimen with cermet coating

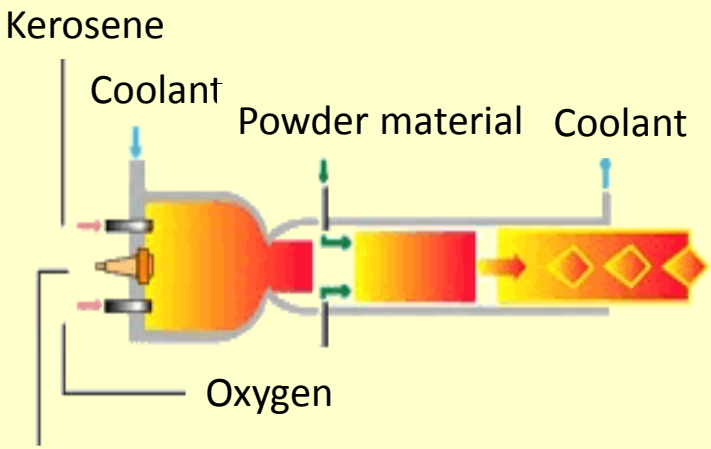

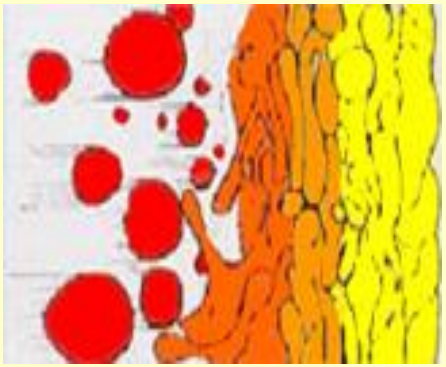

HVOF: High Velocity Oxi-Fuel thermal spraying

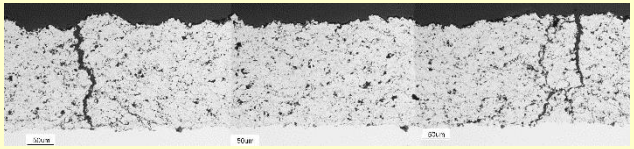

Void and cracks in 40%-carbide cermet

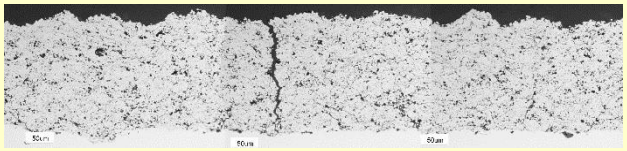

Void and cracks in 75%-carbide cermet

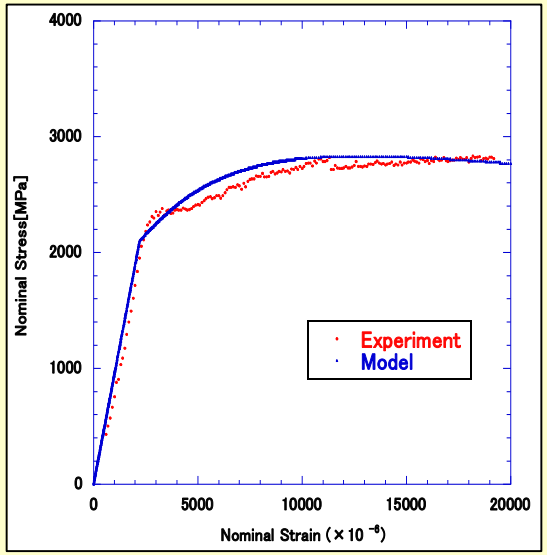

Stress-strain curves for 75%-carbide cermet

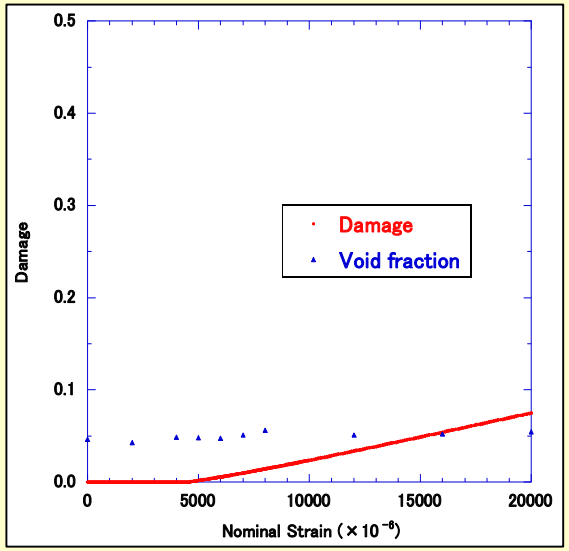

Damage evolution for 75%-carbide cermet

高分子材料の自己修復過程の計算モデリング [42.都井・住吉2009]

Damage evolution equation

$$\dot{D}_F = F(s_{Fi}), \quad i = 1 \sim n_F$$

Healing evolution equation

$$\dot{D}_R = R(s_{Ri}), \quad i = 1 \sim n_R$$

Real damage variable : D

$$\dot{D} = \alpha \dot{D}_F + \beta \dot{D}_R$$

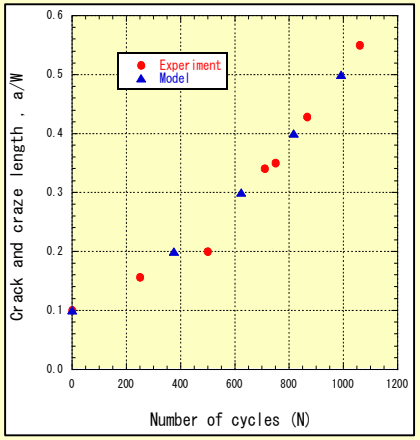

Crack and craze length of PS

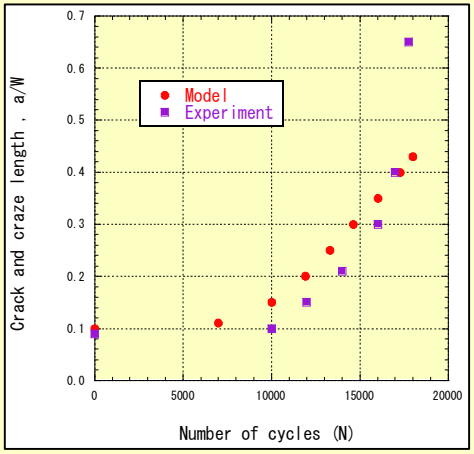

Crack and craze length of PC

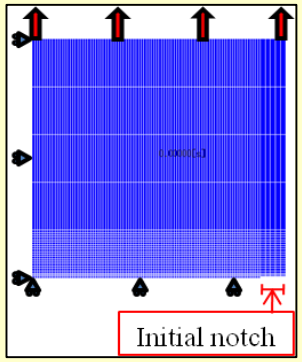

Finite element model

PS

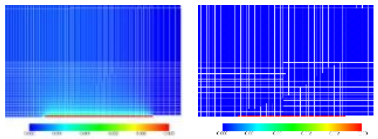

(a) Distribution of damage before and after annealing

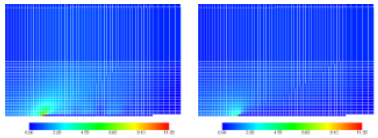

(b) Distribution of stress before and after annealing

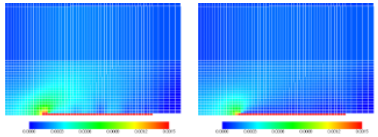

(c) Distribution of strain before and after annealing

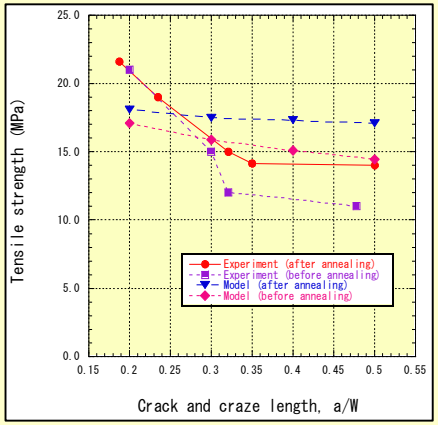

Change in tensile strength of fatigued PS by annealing [*Nemoto*, 2000]

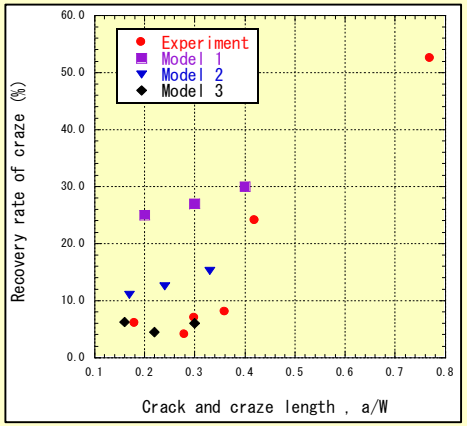

Recovery rate of craze as a function of crack and craze length for PC [*Unno*, 2003]

PC

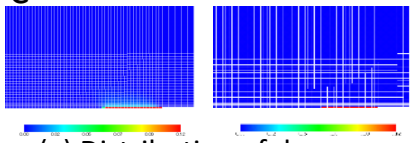

(a) Distribution of damage before and after annealing

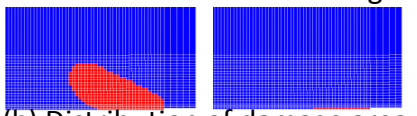

(b) Distribution of damage area before and after annealing

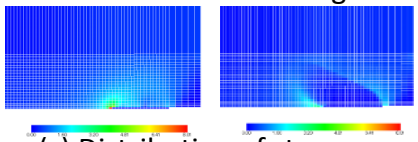

(c) Distribution of stress before and after annealing

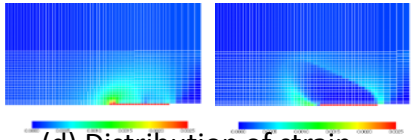

(d) Distribution of strain before and after annealing

高クロム鋼溶接継手のタイプⅣクリープ損傷挙動の解析① [43.都井・高垣・広瀬・高橋2010a]

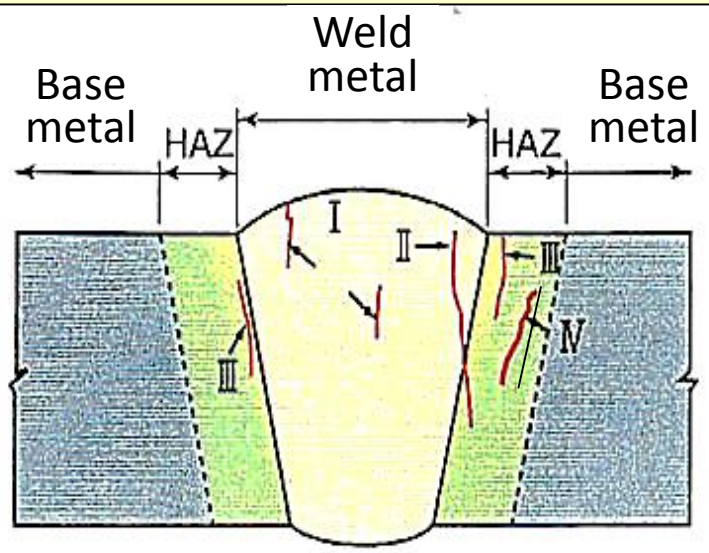

Type Ⅰ： Crack in weld metal

Type Ⅱ： Type Ⅰに分類されるもので溶接金属から熱影響部（HAZ）に進展したき裂

Type Ⅲ： 熱影響部（HAZ）粗粒域に発生した損傷

TypeⅣ： 熱影響部（HAZ）細粒域から部分変態域の範囲に発生した損傷

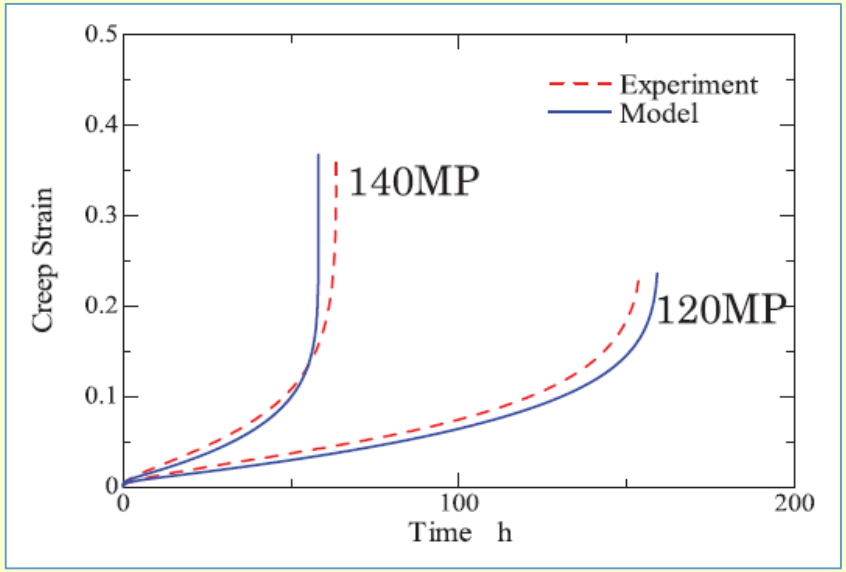

Material modeling of TypeⅣ (600℃, 130MPa)

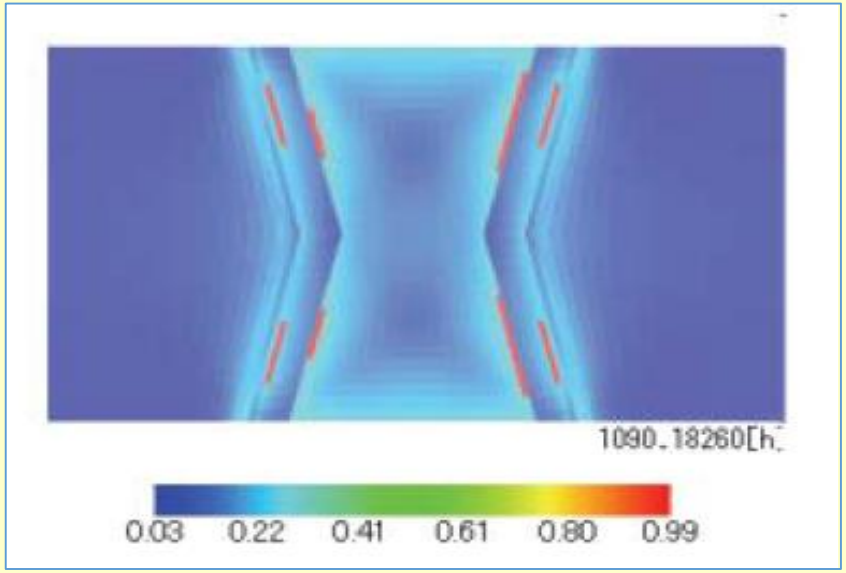

Damage distribution in plate joint [*MHI*]

高クロム鋼溶接継手のタイプⅣクリープ損傷挙動の解析② [44.都井・高垣・広瀬・高橋2010b]

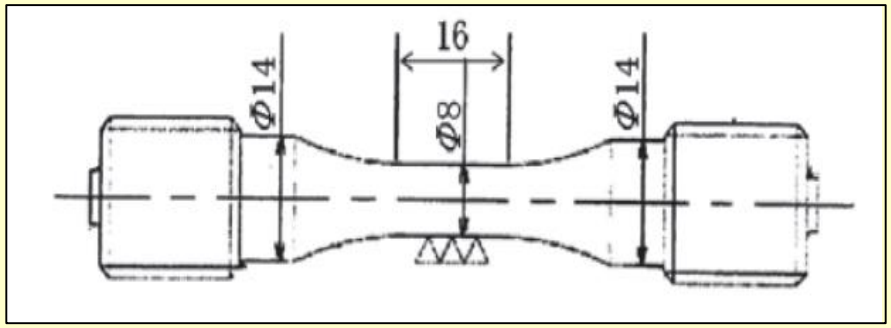

Weld specimen for creep fatigue [*CRIEPI*]

Tempe-rapture [℃]	Strain Range [%]	Hold Time [h]	Creep fatigue lifetime [cycles]	
			Analysis (Fracture)	Experiment (Fracture)
600	1.0	0.0	982 (TypeIV)	1389 (TypeIV)
		0.1	607 (TypeIV)	467 (TypeIV)
		10.0	146 (TypeIV)	250 (TypeIV)

Creep fatigue test results for 9Cr-1Mo steel

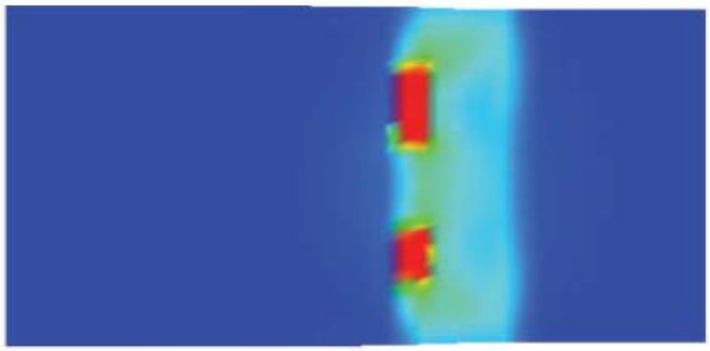

Total damage (max. 0.99)

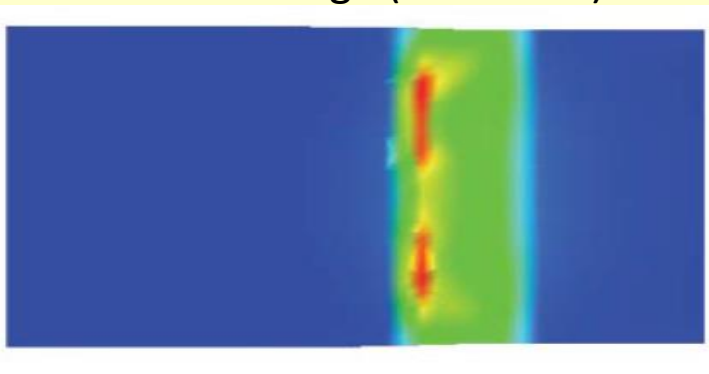

Plastic fatigue damage (max. 0.29)

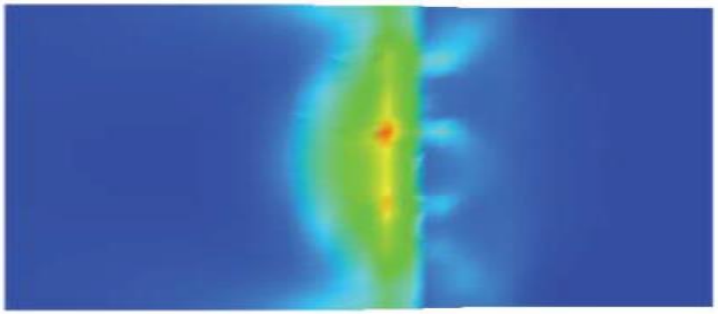

Creep damage (max. 0.08)

連続体損傷力学に基づくディーゼル機関用シリンダヘッドのクリープ疲労寿命解析 [45. 岡・都井2013]

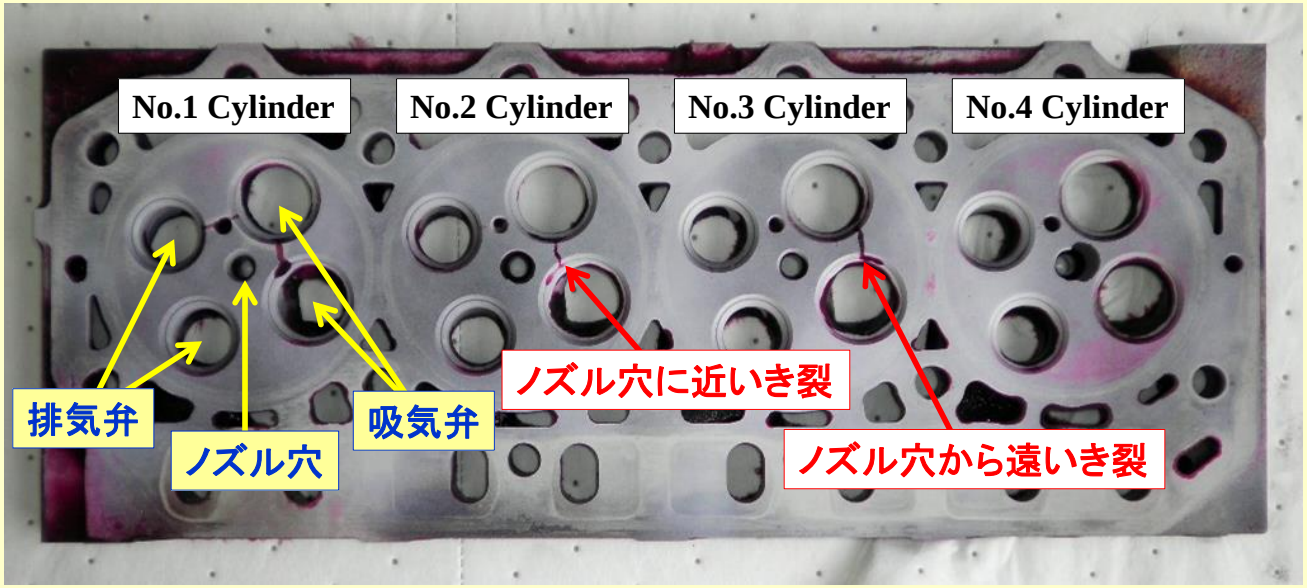

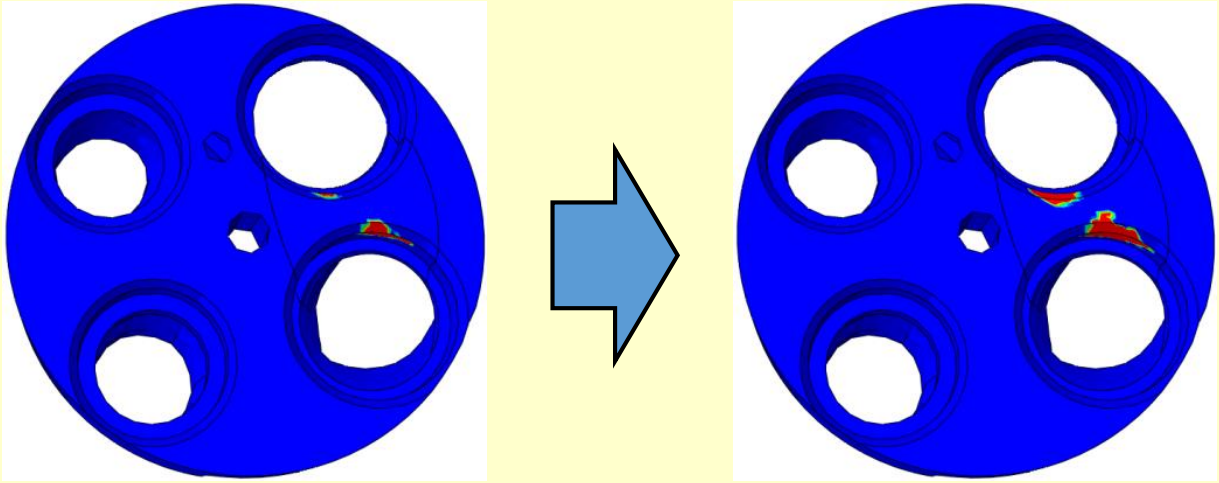

Cycle No. = 1,000　　Cycle No. = 3,000

進展速度が遅く、き裂形状がシャープでないなどの問題はあるが、
実機と同方向にき裂は進展しており、有用性は確認できる。

損傷を考慮した繰返し塑性構成式と低サイクル疲労解析への応用 [46.太田・都井・上田・岡2015]

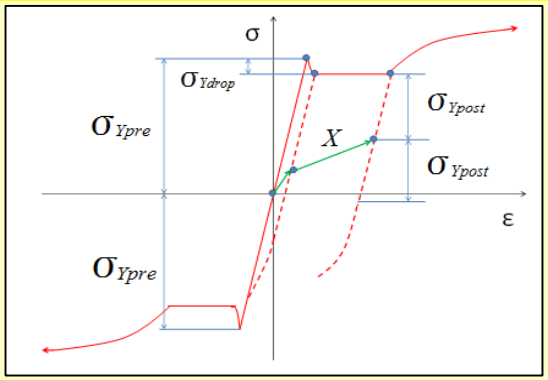

Yield point phenomenon

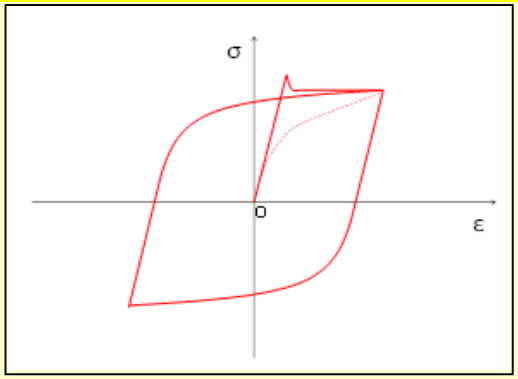

Cyclic plasticity

E[MPa]	210000	X_{∞}^{2}[MPa]	160
ν	0.3	X_{∞}^{3}[MPa]	100
σ_{Ypre}[MPa]	650	m^1	1
σ_{Ydrop}[MPa]	-105	m^2	1
σ_{Ypost}[MPa]	450	m^3	1
R_{∞}	-160	D_{cr}	0.06
b	0.4	s_{pre}	0.6
c	4800	S_{pre}[MPa]	0.6
γ^1	1300	s_{post}	3.4
γ^2	500	S_{post}[MPa]	3.9
γ^3	30	ε_{pD}	0
X_{∞}^{1}[MPa]	270	h	0.1

Material constants

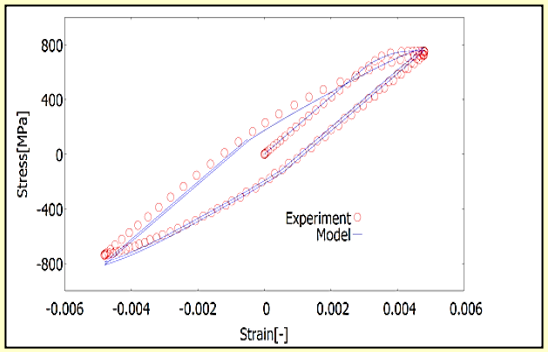

1st and 2nd stress-strain loop
(strain amplitude 0.005)

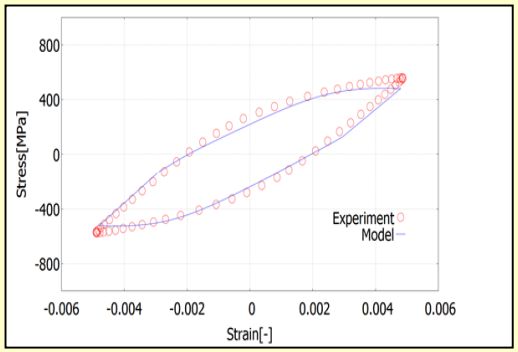

3000th stress-strain loop
(strain amplitude 0.005)

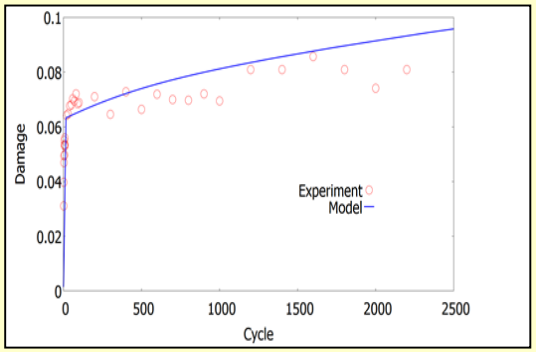

Damage evolution
(strain amplitude 0.005)

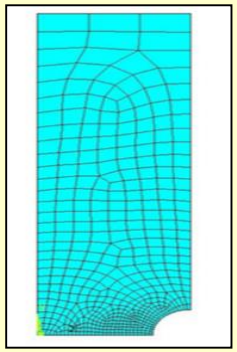

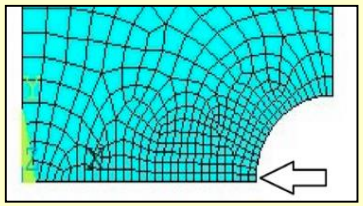

Finite element mesh of a notched bar

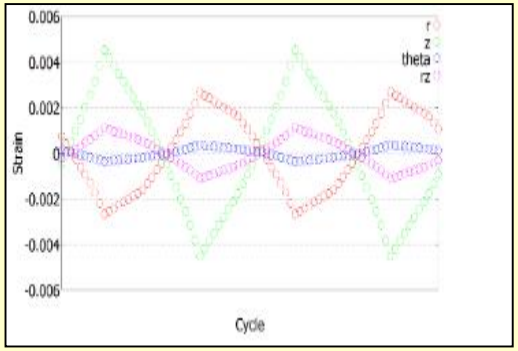

Calculated strains (ANSYS)

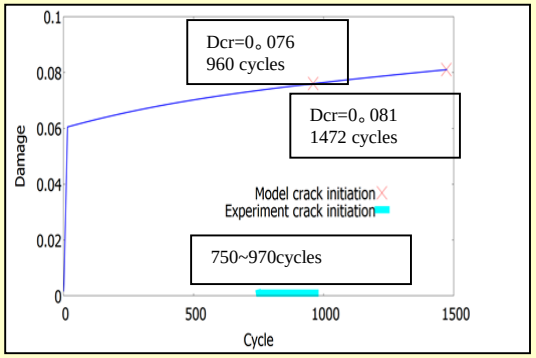

Damage evolution

衛星用スラスタ燃焼器のクリープ疲労解析[57. 升岡・都井2016]

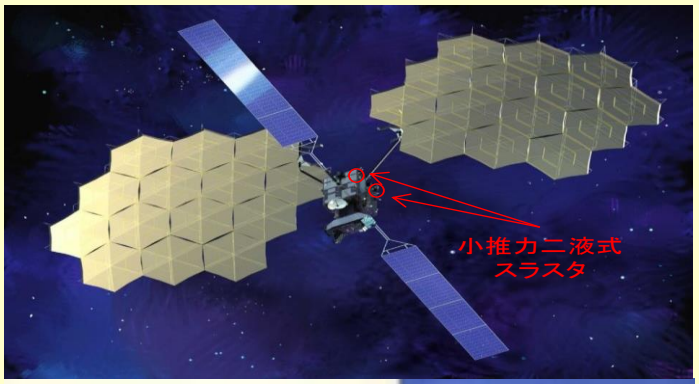

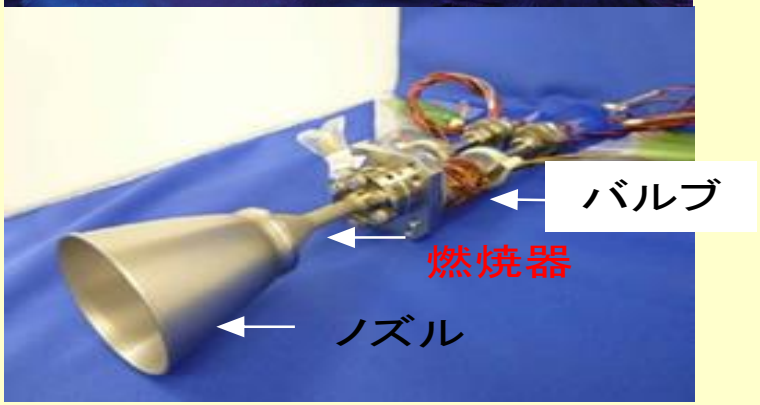

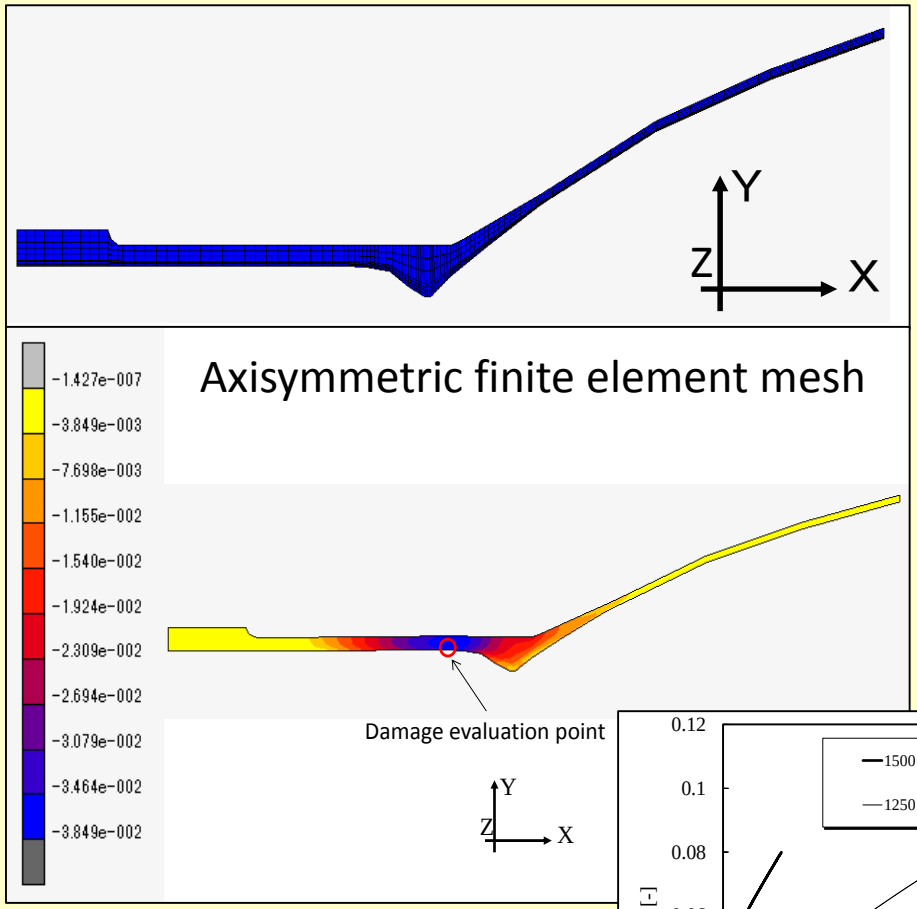

Damage distribution

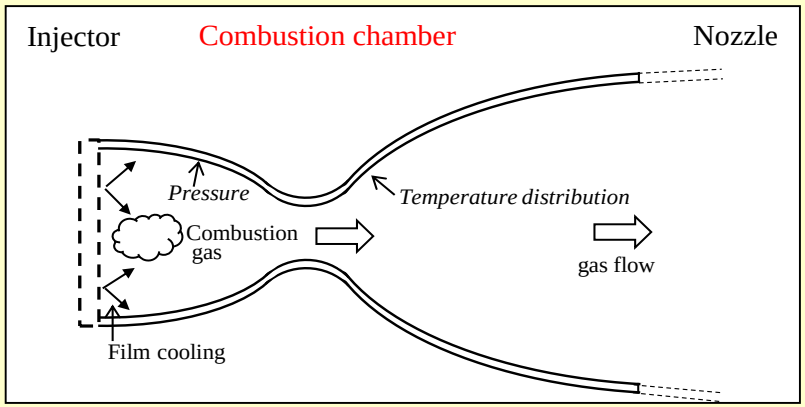

22N Bipropellant thruster

Under combustion

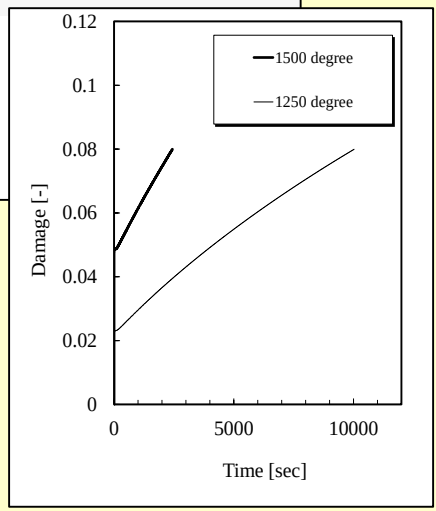

Damage histories